Taylor & Francis
Taylor & Francis Group

RESEARCH PAPER

 OPEN ACCESS Check for updates

Design, synthesis, and biological evaluation of novel ciprofloxacin derivatives as potential anticancer agents targeting topoisomerase II enzyme

Hadeer K. Swedan[a], Asmaa E. Kassab[b], Ehab M. Gedawy[b,c] and Salwa E. Elmeligie[b]

[a]Central Administration of Research and Health Development, Ministry of Health, and Population (MoHP), Cairo, Egypt; [b]Faculty of Pharmacy, Department of Pharmaceutical Organic Chemistry, Cairo University, Cairo, Egypt; [c]Faculty of Pharmacy and Pharmaceutical Industries, Department of Pharmaceutical Chemistry, Badr University in Cairo (BUC), Badr City, Egypt

ABSTRACT

A series of novel ciprofloxacin (CP) derivatives substituted at the N-4 position with biologically active moieties were designed and synthesised. 14 compounds were 1.02- to 8.66-fold more potent than doxorubicin against T-24 cancer cells. Ten compounds were 1.2- to 7.1-fold more potent than doxorubicin against PC-3 cancer cells. The most potent compounds **6**, **7a**, **7b**, **8a**, **9a**, and **10c** showed significant Topo II inhibitory activity (83–90% at $100 \mu M$ concentration). Compounds **6**, **8a**, and **10c** were 1.01- to 2.32-fold more potent than doxorubicin. Compounds **6** and **8a** induced apoptosis in T-24 (16.8- and 20.1-fold, respectively compared to control). This evidence was supported by an increase in the level of apoptotic caspase-3 (5.23- and 7.6-fold, sequentially). Both compounds arrested the cell cycle in the S phase in T-24 cancer cells while in PC-3 cancer cells the two compounds arrested the cell cycle in the G1 phase. Molecular docking simulations of compounds **6** and **8a** into the Topo II active site rationalised their remarkable Topo II inhibitory activity.

GRAPHICAL ABSTRACT
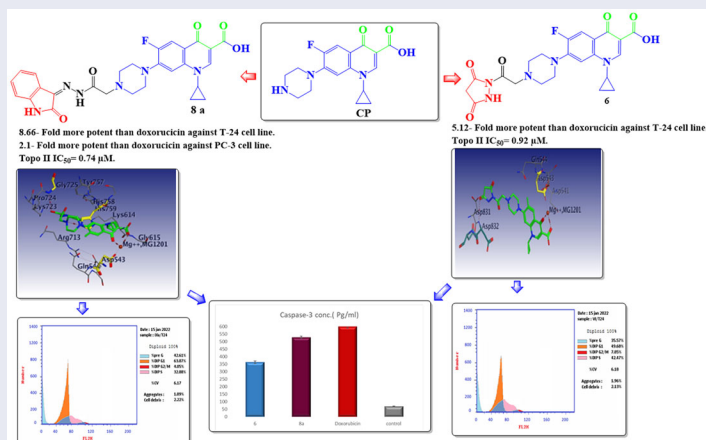
Introduction

Cancer is a very dangerous and life-threatening disease, it is considered one of the most prevalent diseases in the world[1]. The defining characteristic of cancer is metastasis, the leading cause of death from cancer[1–3]. Many antitumor agents are commercially available, but the emergence of acquired drug resistance with severe side effects of these clinically used anticancer drugs poses serious barriers to effective chemotherapy[4]. Therefore, it is recommended to rationally develop new anticancer drugs with fewer side effects.

DNA topological problems arise from the intertwined nature of the DNA double helix structure, which causes tangles and supercoiling of the DNA duplex during the DNA replication and transcription. DNA supercoiling results in torsion that impair the function of DNA or RNA polymerases. Type II topoisomerase enzyme (Topo II) prevents and corrects these types of topological problems via transient double-stranded breaks, causing DNA metabolism to proceed, allowing the cell to efficiently replicate so enabling cellular division and vitality[5–7]. The role of divalent Mg^{2+} ions in Topo II-mediated reactions was recognised as an implication in enzyme-mediated

DNA cleavage reactions. (2) participation in ATPase reactions and functions by providing the enzyme with magnesium–ATP substrate[8]. Topo II enzyme inhibition leads to apoptosis and cell death[9,10], therefore, it is considered a valid strategy in cancer therapy. The presence of topoisomerase enzyme in both mammalian and bacterial cells makes it a pronounced target for antibacterial and anticancer drugs[10,11]. Recently, mammalian Topo II is considered a critical target for anticancer drug development[12–14].

The use of fluoroquinolone derivatives as anti-proliferative agents is of great interest to researchers, as they are less toxic, lower tumour resistance is exerted towards them, and they have less chance of developing secondary tumours. Moreover, they exhibited excellent pharmacological and pharmacokinetic profiles[15–17]. Fluoroquinolones act by inhibiting the Topo II enzyme in both prokaryotic and eukaryotic cells, due to the similarities between the prokaryotic and eukaryotic topoisomerases[18]. A similar mechanism of action characterises several clinically important anti-tumor agents such as etoposide, doxorubicin, amsacrine, or mitoxantrone[19,20]. Recently, a great deal of work has been devoted to the antiproliferative activity of fluoroquinolones and several studies proved them as potent cytotoxic agents[19,21–23]. Ciprofloxacin (CP), a broad-spectrum fluoroquinolone antibiotic, showed anti-proliferative activity against strains of human cancer cells. CP has been reported to pile up in urine and prostate tissues, therefore it is a privileged candidate for the treatment of bladder, and prostate cancers[24]. CP, among fluoroquinolones, is distinguished by strong inhibition of Topo II[25]. Additionally, it can induce the intrinsic apoptotic pathway by creating a double-stranded break in DNA or cell cycle arrest in the S/G2 phase[26,27]. Thus, CP serves as a unique scaffold for the development of novel anticancer agents.

The SAR studies uncovered that fluorine atom, the 1-alkyl, and 1,4-dihydro-4-oxo-quinoline-3-carboxylic acid skeleton are the fundamental pharmacophore lineaments for CP anticancer activity[19,28–31].

Several studies have been conducted to determine the cytotoxic structural features of CP on eukaryotic cells. These studies changed the activity of fluoroquinolones from antibacterial to antitumor activity[32]. Topo II inhibitory activity and pharmacokinetic features of CP are greatly affected by the modification at the piperazinyl N-4 position of the condensed CP[15]. Hence, new fluoroquinolone analogues can be developed by structural modifications at the C-7 position of CP which diminished the zwitterion effect and greatly influenced the hydrophilicity nature leading to the improvement of antiproliferative activity of CP[33–38].

CP hybrids Ia,b[39], II[21], and III[21] (Figure 1) incorporating N-acylarylhydrazone, arylacetamide, and aryl sulphonyl moieties, respectively at the N-4 position of piperazine revealed significant in vitro anti-proliferative activity.

Inspired by all these findings, we have designed a series of novel CP derivatives with essential pharmacophoric features for Topo II inhibition. Our design strategy kept the two coplanar carbonyl groups at positions 3 and 4 of the CP scaffold which is a common structural motif of potent Topo II inhibitors such as merbarone[40], vosaroxin[41], and A-65281[42] (Figure 2). Moreover, this pharmacophore may guarantee the coordination with the Mg^{2+} ion that plays an essential role in promoting the DNA cleavage–rejoining activity of Topo II enzyme[8]. The newly synthesised CP derivatives are featuring various biologically active moieties at the N-4 position of piperazine such as monocyclic heteroaryl scaffolds (pyrazole, pyrazolidine, pyrrolidine, or thiazolidine ring), benzo fused heteroaryl rings (indoline or isoindoline), N-acyl(alkyl or aryl) hydrazone, semicarbazide, thiosemicarbazide or arylacetamide. These moieties are well acknowledged for anti-proliferative activity via different mechanisms such as apoptosis induction, caspase

activation, and DNA inter-chelation[21,43–61]. All these moieties are linked to the piperazine ring of CP via 2, 3, or 4 atoms spacers (Figure 3). We have aimed to explore the impact of such variation at the N-4 position of piperazine of CP core with diverse lipophilic and electronic environments on the anticancer activity and to identify potent anti-proliferative agents. The synthesised CP hybrids were screened for their anti-proliferative activity in vitro against bladder T-24 and prostate PC-3 cancer cell lines. All derivatives were subjected to the determination of their half-maximal inhibitory concentration (IC_{50}) values. The conversion of supercoiled plasmid DNA to relaxed DNA by recombinant Topo II was examined in the presence of each of the most potent compounds 6, 7a, 7b, 8a, 9a, and 10c. The most prominent Topo II inhibitors 6 and 8a were further investigated regarding their effects on cell cycle progression, induction of apoptosis, and level of active caspase-3 in the T-24 cell line.

Materials and methods

Chemistry

General

Melting points were determined on a Griffin apparatus and were uncorrected. Shimadzu IR 435 spectrophotometer (Shimadzu Corp., Kyoto, Japan), Faculty of Pharmacy, Cairo University, Cairo, Egypt, was used to record IR spectra, values were represented in cm^{-1}. ^1H NMR (400 MHz) and ^{13}C NMR (100 MHz) spectra were recorded in ppm on the δ scale and coupling constants (J) were given in Hz on Bruker 400 MHz (Bruker Corp., Billerica, MA, USA) spectrophotometer, Faculty of Pharmacy, Cairo University, Cairo, Egypt. Tetra-methylsilane (TMS) was used as an internal standard. Progress of the reactions was monitored by TLC using pre-coated aluminium sheet silica gel MERCK 60F 254 and was visualised by a UV lamp.

Procedure for the preparation of 1-cyclopropyl-7-(4-(2-ethoxy-2-oxoethyl)piperazin-1-yl)-6-fluoro-4-oxo-1,4-dihydroquinoline-3-carboxylic acid (1). A mixture of ciprofloxacin (1.56 g, 0.005 mol), ethyl chloroacetate (0.61 g, 0.005 mol) and trimethylamine (10 g, 0.1 mol) in dimethylformamide (50 ml) was heated under reflux for 6 h. The reaction mixture was cooled, and the separated solid was filtered, dried, and crystallised from ethanol to give compound 1. MP 190–192 °C; yield 86%[39].

Procedure for the preparation of 1-cyclopropyl-6-fluoro-7-(4-(2-hydrazinyl-2-oxoethyl) piperazin-1-yl)-4-oxo-1,4-dihydroquinoline-3-carboxylic acid (2). A mixture of ester derivative 1 (2.08 g, 0.005 mol) and hydrazine hydrate 99% (1.26 g, 0.025 mol) in absolute ethanol (5 ml) was heated under reflux for 6 h. The reaction mixture was cooled, and the separated solid was filtered, dried, and crystallised from ethanol to give compound 2. MP 226–228 °C (as reported); yield: 75%[39].

Procedure for the preparation of 1-cyclopropyl-6-fluoro-7-(4-(2-(3-methyl-5-oxo-4,5-dihydro-1H-pyrazol-1-yl)-2-oxoethyl)piperazin-1-yl)-4-oxo-1,4-dihydroquinoline-3-carboxylic acid (3). A mixture of the hydrazinyl derivative 2 (0.50 g, 0.001 mol) and ethyl acetoacetate (0.13 g, 0.001 mol) in absolute ethanol (5 ml) was heated under reflux for 6 h. The reaction mixture was cooled, and the separated solid was filtered, dried, and crystallised from ethanol to give compound 3. MP 188–190 °C yield; 60%; IR (KBr) v_{max}: 3549 (OH), 3093 (C–H arom.), 2978 (C–H aliph.), 1730, 1720 (C=O) cm^{-1}; ^1H NMR (DMSO-d$_6$): δ 1.18–1.20 (m, 2H, CH_2 cyclopropyl), 1.30–1.35 (m, 2H,
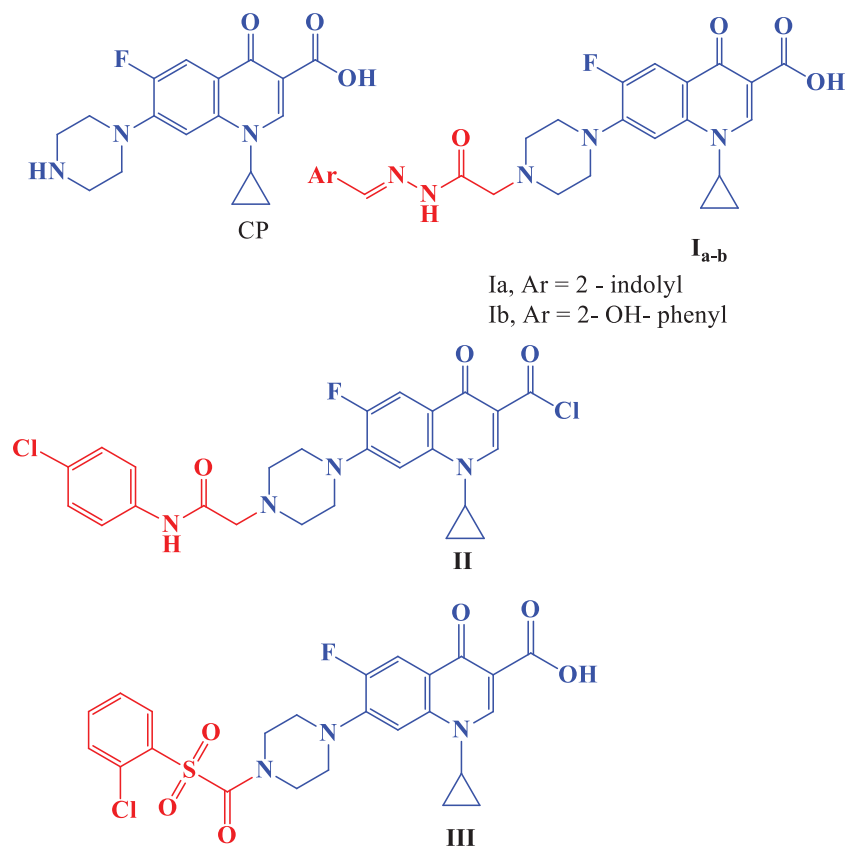
Figure 1. Structures of CP and potent anticancer CP derivatives **I–III**.

Ia, Ar = 2 - indolyl
Ib, Ar = 2- OH- phenyl
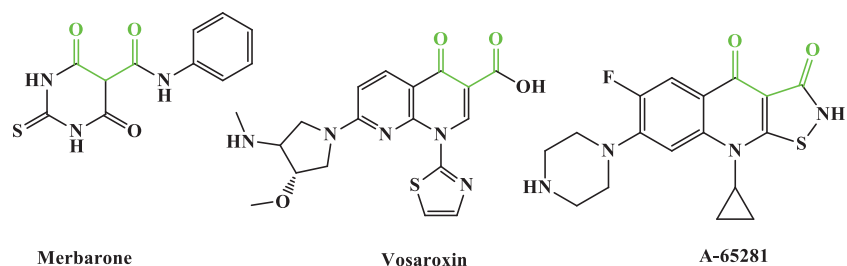
Figure 2. Potent Topo II inhibitors.

Merbarone   Vosaroxin   A-65281

CH₂ cyclopropyl), 2.47 (s, 3H, CH₃C=N), 2.70–2.75 (m, 4H, 2CH₂ piperazine), 3.30–3.40 (m, 4H, 2CH₂ piperazine), 3.40–3.50 (m, 1H, CH cyclopropyl), 3.80 (s, 2H, CH₂ pyrazolone), 4.30 (s, 2H, N-CH₂CO), 7.54 (d, 1H, $J = 8\,Hz$, ArH), 7.85 (d, 1H, $J = 13.6\,Hz$, ArH), 8.60 (s, 1H, C2-H), 15.17 (s, 1H, COOH, D₂O exchangeable) ppm; ¹³C NMR (DMSO-d₆): δ 8.0, 14.6, 36.3, 49.8, 52.0, 58.6, 60.3, 107.1, 111.4, 119.0, 139.6, 145.5, 145.6, 148.4, 152.2, 154.7, 166.3, 170.3, 176.7–176.8 ppm. Anal. Calcd. for C₂₃H₂₄FN₅O₅ (469.47): C, 58.84; H, 5.15; N, 14.92. Found: C, 58.93; H, 5.19; N, 15.22.

Procedure for the preparation of 1-cyclopropyl-6-fluoro-7-(4-(2-(5-imino-3-oxopyrazolidin-1-yl)-2-oxoethyl)piperazin-1-yl)-4-oxo-1,4-dihydroquinoline-3-carboxylic acid (4).

A mixture of hydrazinyl derivative **2** (0.50 g, 0.001 mol) and ethyl cyanoacetate (0.11 g, 0.001 mol) in glacial acetic acid (10 ml) was heated under reflux for 5 h. The reaction mixture was filtered while hot, the filtrate was left to cool, and the separated solid was filtered, washed with water (15 ml) dried and recrystallised from ethanol to give compound **4**. MP 181–183 °C; yield 37%; IR (KBr) ν_{max}: 3541 (OH), 3437, 3417 (2NH), 3059 (C–H arom.), 2870 (C–H aliph.), 1728, 1720 (C=O) cm⁻¹; ¹H NMR (DMSO-d₆): δ 1.25–1.40 (m, 2H, CH₂

cyclopropyl), 1.60–1.65 (m, 2H, CH₂ cyclopropyl), 2.80–2.95 (m, 4H, 2CH₂ piperazine), 3.36–3.41 (m, 4H, 2CH₂ piperazine), 3.44 (s, 2H, NCH₂O), 3.80–3.90 (m, 1H, CH cyclopropyl), 3.86 (s, 2H, CH₂ pyrazalone) 7.57 (d, 1H, ArH), 7.90 (d, 1H, $J = 8\,Hz$, ArH), 8.66 (s, 1H, C2-H), 9.68 (s, 1H, NH, D₂O exchangeable), 9.75 (s, 1H, NH, D₂O exchangeable), 15.19 (s, 1H, COOH D₂O exchangeable) ppm; ¹³C NMR (DMSO-d₆): δ 5.9, 12.5, 24.0, 34.2, 43.7, 47.5, 104.6, 109.3, 115.3, 116.8, 122.5, 137.5, 143.4, 146.2, 163.6, 164.2, 168.2, 169.5, 174.6 ppm. Anal. Calcd. for C₂₂H₂₃FN₆O₅ (470.45): C, 56.17; H, 4.93; N, 17.86. Found: C, 56.40; H, 4.81; N, 18.05.

Procedure for the preparation of 1-cyclopropyl-7-(4-(2-(3,5-dimethyl-1H-pyrazol-1-yl)-2-oxoethyl)piperazin-1-yl)-6-fluoro-4-oxo-1,4-dihydro-quinoline-3-carboxylic acid (5).

A mixture hydrazinyl derivative **2** (0.50 g, 0.001 mol) and acetylacetone (0.1 g, 0.001 mol) in absolute ethanol (5 ml) was heated under reflux for 6 h. The reaction mixture was cooled, and the separated solid was filtered, dried, and crystallised from ethanol to give compound **5**. MP: 185–187 °C; yield: 60%; IR (KBr) ν_{max}: 3444 (OH), 3055 (C–H arom.), 2912 (C–H aliph.), 1730, 1728, 1720 (C=O) cm⁻¹; ¹H NMR (DMSO-d₆): δ 1.15–1.20 (m, 2H, CH₂ cyclopropyl), 1.30–1.35 (m, 2H, CH₂
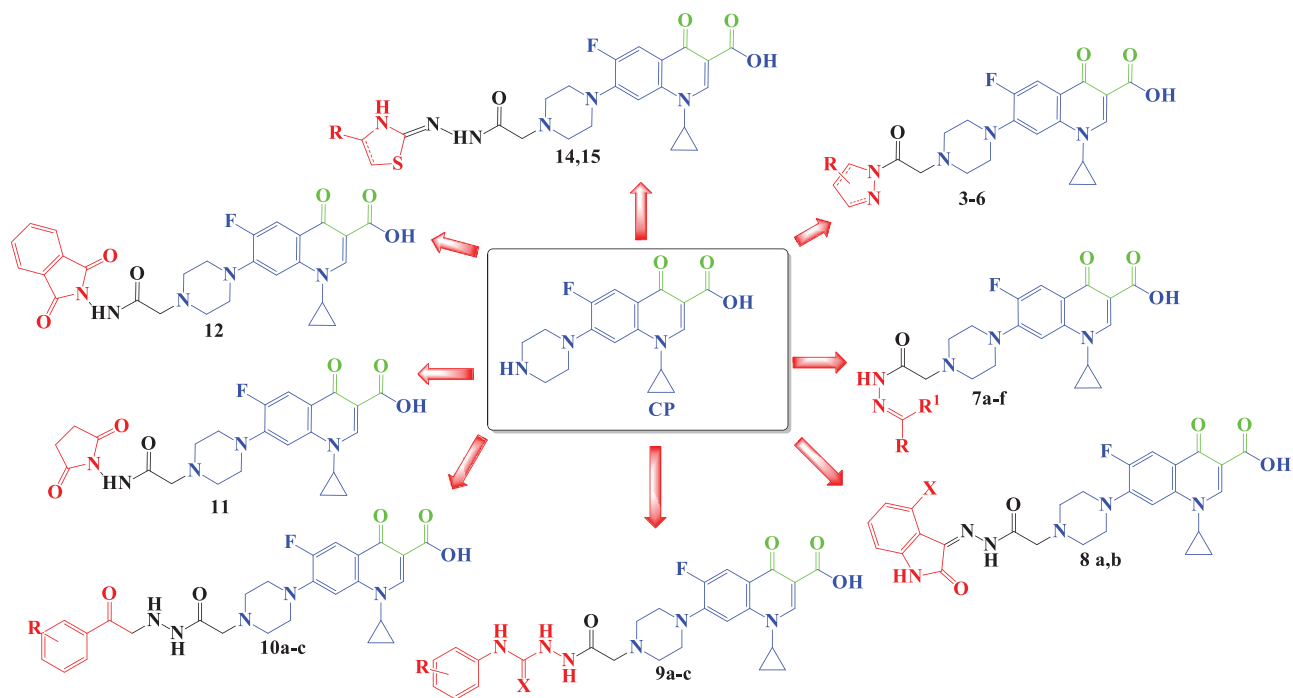
Figure 3. Design strategy for the synthesised CP hybrids.

cyclopropyl), 2.75–2.80 (m, 7H, 2CH$_2$, CH$_3$), 2.90 (s, 3H, CH$_3$), 3.30–3.35 (m, 4H, 2CH$_2$ piperazine), 3.40–3.50 (m, 1H, CH cyclopropyl), 3.80 (s, 2H, CH$_2$CO), 7.55 (d, 1H, ArH), 7.88 (d, 1H, ArH), 7.90 (s, 1H, CH pyrazole), 8.63 (s, 1H, C2-H), 15.16 (s, 1H, COOH, D$_2$O exchangeable) ppm; ^{13}C NMR (DMSO-d$_6$): δ 8.0, 14.6, 19.0, 36.3, 49.8, 52.0, 58.6, 106.8, 107.1, 111.2, 111.4, 118.9, 139.6, 145.6, 148.3, 152.2, 154.6, 166.3, 170.3, 176.7 ppm. Calcd. for C$_{24}$H$_{26}$FN$_5$O$_4$ (467.49): C, 61.66; H, 5.61; N, 14.98. Found: C, 61.92; H, 5.72; N, 15.17.

Procedure for the preparation of 1-cyclopropyl-7-(4-(2-(3,5-dioxo-pyrazolidin-1-yl)-2-oxoethyl)piperazin-1-yl)-6-fluoro-4-oxo-1,4-dihy-droquinoline-3-carboxylic acid (6). A mixture of hydrazinyl derivative **2** (0.20 g, 0.0005 mol) in sodium ethoxide (0.034 g atomic weight of sodium in 17 ml absolute ethanol), diethyl malonate (0.1 g, 0.0008 mol) was heated under reflux for 7 h. The reaction mixture was cooled, and the separated solid was filtered, washed with water (5 ml) dried, and crystallised from ethanol to give compound **6**. MP: 140–142 °C; yield: 35%; IR IR (KBr) v_{max}: 3583 (OH), 3441 (NH), 3008 (C–H arom.), 2958 (C–H aliph.), 1680, 1660 (C=O) cm^{-1}; ^{1}H NMR (DMSO-d$_6$): δ 1.15–1.30 (m, 4H, 2CH$_2$ cyclopropyl), 2.70–2.80 (m, 4H, 2CH$_2$ piperazine), 2.90 (s, 2H, CH$_2$ pyrazolone), 3.20–3.25 (m, 4H, 2CH$_2$ piperazine), 3.35 (s, 2H, CH$_2$CO), 3.65 (s, 1H, NH, D$_2$O exchangeable), 3.95–4.00 (m, 1H, CH cyclopropyl), 7.54 (d, 1H, ArH), 7.85 (d, 1H, ArH), 8.59 (s, 1H, C2-H) ppm; ^{13}C NMR (DMSO-d$_6$): δ 8.0, 14.6, 15.3, 36.3, 49.8, 60.3, 106.8, 117.6, 119.0, 130.1, 133.2, 148.3, 152.2, 154.7, 160.0, 166.3, 168.5, 170.3, 176.8 ppm. Anal. Calcd. for C$_{22}$H$_{22}$FN$_5$O$_6$ (471.44): C, 56.90; H, 4.70; N, 14.86. Found: C, 56.11; H, 4.68; N, 14.84.

General procedure for the preparation of 7-(4-(-1-(substituted)e-thylidene)hydrazine carbonyl)methyl)piperazin-1-yl)-1-cyclopropyl-6-fluoro-4-oxo-1,4-dihydroquinoline-3-carboxylic acid (7a–f)
A mixture of hydrazinyl derivative **2** (0.50 g, 0.001 mol), the appro-priate ketone (0.001 mol), and glacial acetic acid (1 ml) in absolute ethanol (5 ml) was heated under reflux for 6 h. The reaction mix-ture was cooled, and the separated solid was filtered, dried, and recrystallised from ethanol to give compounds **7a–f**.

7-(4-(2-(2-Cyclohexylidenehydrazinyl)-2-oxoethyl)piperazin-1-yl)-1-cyclopropyl-6-fluoro-4-oxo-1,4-dihydroquinoline-3-carboxylic acid (7a). M.P.: 256–258 °C; yield: 65%; IR (KBr) v_{max}: 3497 (OH), 3417 (NH), 3043 (C–H arom.), 2981, 2962 (C–H aliph.) cm^{-1}; ^{1}H NMR (DMSO-d$_6$): δ 1.18–1.25 (m, 2H, CH$_2$ cyclopropyl), 1.31–1.33 (m, 2H, CH$_2$ cyclopropyl), 2.91–2.93 (m, 2H, CH$_2$ cyclohexylidene) 3.24–3.25 (m, 4H, 2CH$_2$ cyclohexylidene), 3.40–3.50 (m, 1H, CH cyclopropyl), 3.60–3.70 (m, 4H, 2CH$_2$ cyclohexylidene), 3.82 (s, 2H, CH$_2$CO) 7.55 (d, 1H, J = 8 Hz, ArH), 7.87 (d, 1H, J = 12 Hz, ArH), 8.13 (s, 1H, NH, D$_2$O exchangeable), 8.65 (s, 1H, C2-H) ppm; ^{13}C NMR (DMSO-d$_6$): δ 8.0, 19.0, 34.2, 36.2, 45.8, 51.0, 51.1, 57.0, 77.0, 106.4, 107.2, 111.3, 118.7, 139.6, 146.1, 148.2, 166.4, 152.1, 154.6, 176.7 ppm. Anal. Calcd. for C$_{25}$H$_{30}$FN$_5$O$_4$ (483.54): C, 62.10; H, 6.25; N, 14.48. Found: C, 62.12; H, 6.28; N, 14.46.

7-(4-(2-(2-(1-(4-Chlorophenyl)ethylidene)hydrazinyl)-2-oxoethyl)-piperazin-1-yl)-1-cyclopropyl-6-fluoro-4-oxo-1,4-dihydroquinoline-3-carboxylic acid (7b). M.P.: 178–180 °C; yield 75%; IR (KBr) v_{max}: 3444 (OH), 3298 (NH), 3078 (C–H arom.), 2924, 2827 (C–H aliph.), 1705 (C=O) cm^{-1}; ^{1}H NMR (DMSO-d$_6$): δ 1.19–1.23 (m, 2H, CH$_2$ cyclopropyl), 1.33–1.40 (m, 2H, CH$_2$ cyclopropyl), 2.18 (s, 3H, CH$_3$), 2.25–2.30 (m, 4H, 2CH$_2$ piperazine), 2.70–2.90 (m, 4H, 2CH$_2$ pipera-zine), 3.05 (s, 2H, CH$_2$CO), 3.78–3.80 (m, 1H, CH cyclopropyl), 7.50–7.52 (m, 3H, ArH), 7.82–8.00 (m, 3H, ArH), 8.6 (s, 1H, C2-H), 10.42, 10.66 (2 s, 1H, NH, D$_2$O exchangeable), 15.22 (s, 1H, COOH, D$_2$O exchangeable) ppm. Anal. Calcd. for C$_{27}$H$_{27}$ClFN$_5$O$_4$ (539.99): C, 60.06; H, 5.04; N, 12.97. Found: C, 60.13; H, 5.18; N, 12.92.

7-(4-(2-(2-(1-(4-Aminophenyl)ethylidene)hydrazinyl)-2-oxoethyl)-piperazin-1-yl)-1-cyclopropyl -6-fluoro-4-oxo-1,4-dihydroquinoline-3-carboxylic acid (7c). M.P.: 173–175; yield 70%; IR (KBr) v_{max}: 3421 (OH), 3356, 3232 (NH, NH$_2$), 3051 (C–H arom.), 2974 (C–H aliph.), 1730, 1728 (C=O) cm^{-1}; ^{1}HNMR (DMSO-d$_6$): δ 1.19–1.22 (m, 2H, CH$_2$ cyclopropyl), 1.26–1.33 (m, 2H, CH$_2$ cyclopropyl), 1.84–1.87 (m, 1H, CH cyclopropyl), 2.80–2.93 (m, 4H, 2CH$_2$ piperazine), 3.46–3.92 (m, 7H, 2CH$_2$ piperazine, CH$_3$), 3.87 (s, 2H, CH$_2$CO), 4.20 (s, 2H,

NH$_2$, D$_2$O exchangeable), 7.11 (s, 1H, NH, D$_2$O exchangeable) 7.54 (d, 3H, ArH), 7.94 (d, 3H, ArH), 8.68 (s, 1H, C2-H), 11.23 (s, 1H, OH exchangeable by D$_2$O) ppm. Anal. Calcd. for C$_{27}$H$_{29}$FN$_6$O$_4$ (520.56): C, 62.30; H, 5.62; N, 16.14. Found: C, 62.28; H, 5.57; N, 16.16.

1-Cyclopropyl-6-fluoro-7-(4-(2-(2-(1-(2-hydroxyphenyl)ethylidene)-hydrazinyl)-2-oxoethyl)piperazin-1-yl)-4-oxo-1,4-dihydroquinoline-3-carboxylic acid (7d).

M.P.: 166–168; yield 80%; IR (KBr) v_{max}; 3545 (OH), 3417 (NH), 3059 (C–H arom.), 2912 (C–H aliph.), 1728, 1705 (C=O) cm^{-1}; ^{1}H NMR (DMSO-d$_6$): δ 1.18–1.22 (m, 2H, CH$_2$ cyclopropyl), 1.32–1.33 (m, 2H, CH$_2$ cyclopropyl), 2.53 (s, 3H, CH$_3$), 2.75–2.80 (m, 4H, CH$_2$ piperazine), 3.33–3.45 (m, 6H, 2CH$_2$ piperazine, CH$_2$CO), 3.81–3.90 (m, 1H, CH cyclopropyl), 6.95 (d, 2H, ArH), 7.40 (t, 1H, ArH), 7.55 (d, 1H, ArH), 7.76 (d, 1H, ArH), 7.89 (d, 1H, ArH), 8.64 (s, 1H, C2-H), 12.93 (s, 1H, NH, D$_2$O exchangeable), 13.12 (s, 1H, OH, D$_2$O exchangeable) 15.20 (s, 1H, COOH, D$_2$O exchangeable) ppm. ^{13}C NMR (DMSO-d$_6$): δ 8.0, 15.3, 36.2, 49.8, 52.0, 60.3, 106.8, 107.1, 111.4, 117.6, 118.9, 119.5, 130.1, 133.2, 139.6, 145.5, 148.3, 152.1, 154.6, 160.0, 166.3, 168.6, 170.3, 176.7 ppm. Anal. Calcd. for C$_{27}$H$_{28}$FN$_5$O$_5$ (521.56): C, 62.18; H, 5.41; N, 13.43. Found: C, 61.96; H, 5.70; N, 13.62.

1-Cyclopropyl-6-fluoro-4-oxo-7-(4-(2-oxo-2-(2-(1-(thiophen-2-yl)ethylidene)hydrazinyl)ethyl)piperazin-1-yl)-1,4-dihydroquinoline-3-carboxylic acid (7e).

M.P.: 245–247; yield 85%; IR (KBr) v_{max}: 3441 (OH), 3271 (NH), 3082 (C–H arom.), 2947 (C–H aliph.), 1730, 1728 (C=O) cm^{-1}; ^{1}H NMR (DMSO-d$_6$): δ 1.15–1.20 (m, 2H, CH$_2$ cyclopropyl), 1.25–1.30 (m, 2H, CH$_2$ cyclopropyl), 2.40 (s, 3H, CH$_3$), 2.60–2.65 (m, 4H, 2CH$_2$ piperazine), 2.70–2.80 (m, 4H, 2CH$_2$ piperazine), 3.27 (s, 2H, CH$_2$ CO), 3.85–3.90 (m, 1H, CH cyclopropyl), 7.05–7.15 (m, 2H, ArH), 7.50–7.70 (m, 2H, ArH), 7.95 (d, 1H, ArH), 8.65 (s, 1H, C2-H), 8.99, 9.67 (2 s, 1H, NH, D$_2$O exchangeable), 15.19 (s, 1H, COOH, D$_2$O exchangeable) ppm. ^{13}C NMR (DMSO-d$_6$): δ 8.0, 14.6, 36.3, 49.7, 49.9, 52.6, 106.8, 107.7, 111.2, 118.9, 119.0, 127.9, 128.5, 139.6, 143.5, 144.0, 145.6, 148.3, 154.6, 168.5, 171.5, 176.7 ppm. Anal. Calcd. for C$_{25}$H$_{26}$FN$_5$O$_4$S (511.57): C, 58.70; H, 5.12; N, 13.69. Found: C, 58.63; H, 5.15; N, 13.72.

7-(4-(2-(2-(1-(5-Chlorothiophen-2-yl)ethylidene)hydrazinyl)-2-oxoethyl)piperazin-1-yl)-1-cyclopropyl-6-fluoro-4-oxo-1,4-dihydroquinoline-3-carboxylic acid (7f).

M.P.: 286–288; yield 85%; IR (KBr) v_{max}: 3456 (OH), 3275 (NH), 3059 (C–H arom.), 2924 (C–H aliph.), 1730, 1728 (C=O) cm^{-1}; ^{1}H NMR (DMSO-d$_6$): δ 1.10–1.20 (m, 2H, CH$_2$ cyclopropyl), 1.27–1.33 (m, 2H, CH$_2$ cyclopropyl), 2.38 (s, 3H, CH$_3$), 2.70–2.74 (m, 4H, 2CH$_2$ piperazine), 3.30–3.42 (m, 6H, 2CH$_2$ piperazine, CH$_2$CO), 3.70–3.90 (m, 1H, CH cyclopropyl), 7.18–7.20 (m, 2H, ArH), 7.56 (d, 1H, ArH), 7.75 (d, 1H, ArH), 8.65 (s, 1H, C2-H), 10.30, 10.55 (2 s, NH, D$_2$O exchangeable), 15.19 (s, 1H, COOH, D$_2$O exchangeable) ppm; ^{13}C NMR (DMSO-d$_6$): δ 8.0, 14.6, 19.0, 36.3, 49.8, 56.4, 106.8, 107.1, 111.2, 111.4, 117.6, 119.0, 139.6, 145.5, 148.3, 152.2, 154.7, 166.3, 168.5, 170.3, 176.7 ppm. Anal. Calcd. for C$_{25}$H$_{25}$ClFN$_5$O$_4$S (546): C, 54.99; H, 4.61; N,12.83. Found: C, 54.92; H, 4.63; N,12.80.

General procedure for the preparation of 7-(4-((N'-(4-substituted-2-oxo-2,3-dihydro-1H-indol-3-ylidene)hydrazine carbonyl)methyl)-piperazin-1-yl)1-cyclopropyl-6-fluoro-4-oxo-1,4-dihydroquinoline-3-carboxylic acid (8a–b)

A mixture of hydrazinyl derivative 2 (0.50 g, 0.001 mol), substituted isatin (0.001 mol) and glacial acetic acid (1 ml) in absolute ethanol (5 ml) was heated under reflux for 7 h. The reaction mixture was cooled, and the separated solid was filtered, dried, and recrystallised from ethanol to give compounds 8a–b.

1-Cyclopropyl-6-fluoro-4-oxo-7-(4-(2-oxo-2-(2-(2-oxoindolin-3-ylidene)hydrazinyl)ethyl) piperazin-1-yl)-1,4-dihydroquinoline-3-carboxylic acid (8a).

M.P.: 186–188; yield 85%; IR (KBr) v_{max}: 3441 (OH), 3240 (NH), 3051 (C–H arom.), 2974 (C–H aliph.), 1730, 1720, 1712 (C=O) cm^{-1}. ^{1}H NMR (DMSO-d$_6$): δ 1.02–1.05 (m, 2H, CH$_2$ cyclopropyl), 1.17–1.20 (m, 2H, CH$_2$ cyclopropyl), 2.72–2.74 (m, 4H, 2CH$_2$ piperazine), 3.29–3.31 (m, 4H, 2CH$_2$ piperazine), 3.45 (s, 2H, CH$_2$CO), 3.75–3.85 (m, 1H, CH cyclopropyl), 6.85–6.88 (m, 1H, ArH), 7.03–7.05 (m, 1H, ArH), 7.36–7.45 (m, 2H, ArH), 7.50 (d, 1H, ArH), 7.90 (d, 1H, ArH), 8.65 (s, 1H, C2-H), 10.96, 11.10 (2 s, 1H, NH, D$_2$O exchangeable), 13.84 (s, 1H, NH, D$_2$O exchangeable), 15.91 (s, 1H, COOH, D$_2$O exchangeable) ppm. ^{13}C NMR (DMSO-d$_6$): δ 8.0, 14.6, 36.3, 49.8, 58.6, 60.3, 106.8, 111.5, 112.6, 118.2, 118.9, 123.2, 125.1, 128.6, 134.8, 138.8, 139.5, 145.6, 151.1, 152.1, 154.6, 166.3, 170.3, 176.7, 184.8 ppm. Anal. Calcd. for C$_{27}$H$_{25}$FN$_6$O$_5$ (532.52): C, 60.90; H, 4.73; N, 15.78. Found: C, 60.88; H, 4.71; N, 15.76.

7-(4-(2-(2-(4-Bromo-2-oxoindolin-3-ylidene)hydrazinyl)-2-oxoethyl)-piperazin-1-yl)-1-cyclopropyl-6-fluoro-4-oxo-1,4-dihydro-quinoline-3-carboxylic acid (8b).

M.P.: 263–265; yield 70%; IR (KBr) v_{max}: 3498 (OH), 3200, 3174 (NH), 3078 (C–H arom.), 2916 (C–H aliph.), 1720, 1700, 1697 (C=O) cm^{-1}; ^{1}H NMR (DMSO-d$_6$): δ 1.20–1.23 (m, 2H, CH$_2$ cyclopropyl), 1.30–1.35 (m, 2H, CH$_2$ cyclopropyl), 2.74–2.77 (m, 4H, 2CH$_2$ piperazine), 3.34–3.35 (m, 4H, 2CH$_2$ piperazine), 3.45 (s, 2H, CH$_2$CO), 3.80–3.90 (m, 1H, CH cyclopropyl), 6.85–6.90 (m, 1H, ArH), 7.57–7.65 (m, 2H, ArH), 7.72 (d, 1H, ArH), 7.89 (d, 1H, $J = 12$ Hz, ArH), 8.60 (s, 1H, C2-H), 11.14, 11.26 (2 s, 1H, NH, D$_2$O exchangeable), 13.83 (s, 1H, NH, D$_2$O exchangeable), 15.21 (s, 1H, COOH, D$_2$O exchangeable) ppm. ^{13}C NMR (DMSO-d$_6$): δ 8.0, 14.6, 49.8, 52.0, 58.6, 60.3, 106.9, 107.2, 111.2, 111.5, 114.7, 119.0, 120.0, 127.3, 139.6, 140.4, 145.5, 145.6, 148.4, 150.0, 159.4, 166.3, 170.3, 176.8, 183.6 ppm. Anal. Calcd. for C$_{27}$H$_{24}$BrFN$_6$O$_5$ (611.42): C, 53.04; H, 3.96; N, 13.75. Found: C, 57.13; H, 4.15; N, 14.18.

General procedure for the preparation of 7-(4-(substituted)phenyl)-carbamoyl)amino)carbamoyl)methyl)piperazin-1-yl)-1-cyclopropyl-6-fluoro-4-oxo-1,4-dihydroquinoline-3-carboxylic acid (9a-c)

A mixture of hydrazinyl derivative 2 (0.50 g, 0.001 mol), substituted phenyl isocyanate or phenyl isothiocyanate (0.001 mol), and glacial acetic acid (1 ml) in absolute ethanol (15 ml) was heated under reflux for 7 h. The reaction mixture was cooled, and the separated solid was filtered, dried, and recrystallised from ethanol to give compounds 9a–c.

7-(4-(2-(2-((4-Chloro-3-(trifluoromethyl)phenyl)carbamoyl)-hydrazinyl)-2-oxoethyl) piperazin-1-yl)-1-cyclopropyl-6-fluoro-4-oxo-1,4-dihydroquinoline-3-carboxylic acid (9a).

M.P.: 186–188; yield 65%; IR (KBr) v_{max}: 3437 (OH), 3414 (NH), 3055 (C–H arom.), 2908 (C–H aliph.), 1730, 1728 (C=O) cm^{-1}; ^{1}H NMR (DMSO-d$_6$): δ 1.04–1.08 (m, 2H, CH$_2$ cyclopropyl), 1.32–1.33 (m, 2H, CH$_2$ cyclopropyl), 2.65 (s, 2H, CH$_2$CO), 2.70–2.77 (m, 4H, 2CH$_2$ piperazine), 3.30–3.45 (m, 4H, 2CH$_2$ piperazine), 3.80–3.90 (m, 1H, CH cyclopropyl), 7.56–7.70 (m, 3H, ArH), 7.87–8.15 (m, 2H, ArH), 8.65 (s, 1H, C2-H), 9.30 (s, 1H, NH, D$_2$O exchangeable), 9.50 (s, 1H, NH, D$_2$O exchangeable), 10.10 (s, 1H, NH, D$_2$O exchangeable), 15.07 (s, 1H, COOH, D$_2$O exchangeable) ppm; ^{13}C NMR (DMSO-d$_6$): δ 8.3, 14.6, 49.8, 52.0, 60.3, 106.8, 106.9, 107.1, 111.2, 111.4, 118.9, 119.0, 139.6, 145.5, 145.6, 148.3, 152.2, 154.7, 166.3, 170.3, 176.7, 176.8 ppm. Anal. Calcd. for

$C_{27}H_{25}ClF_4N_6O_5$ (624.97): C, 51.89; H, 4.03; N, 13.45. Found: C, 52.17; H, 4.19; N, 13.71.

7-(4-(2-(2-((2-Chloro-6-methylphenyl)carbamoyl)hydrazinyl)-2-oxoe-thyl)piperazin-1-yl)-1-cyclopropyl-6-fluoro-4-oxo-1,4-dihydro-quin-oline-3-carboxylic acid (9b).

M.P.: 285–287; yield 83%; IR (KBr) v_{max}: 3572 (OH), 3441 (NH), 3051 (C–H arom.), 2904 (C–H aliph.), 1730, 1728 (C=O) cm^{-1}. ^{1}H NMR (DMSO-d$_6$): δ 1.15–1.25 (m, 4H, 2CH$_2$ cyclopropyl), 2.20–2.25 (m, 11H, 4CH$_2$ piperazine, CH$_3$), 3.34 (s, 2H, CH$_2$CO), 4.80–4.90 (m, 1H, CH cyclopropyl), 7.17–7.24 (m, 3H, ArH), 7.33–7.35 (m, 3H, ArH), 8.94 (brs, 3H, 3NH, D$_2$O exchangeable). ^{13}C NMR (DMSO-d$_6$): δ 8.0, 18.8, 36.3, 44.1, 49.8, 49.9, 106.9, 107.8, 111.4, 119.0, 127.7, 129.2, 133.1, 135.6, 139.3, 145.4, 145.5, 148.2, 152.1, 154.4, 155.6, 166.3, 176.6, 176.7 ppm. Anal. Calcd. for $C_{27}H_{28}ClFN_6O_5$ (571): C, 56.79; H, 4.94; N, 14.72. Found: C, 57.05; H, 5.12; N, 14.98.

1-Cyclopropyl-6-fluoro-7-(4-(2-(2-((4-methoxyphenyl)carbamo-thio-yl)hydrazinyl)-2-oxoethyl)piperazin-1-yl)-4-oxo-1,4-dihydroquino-line-3-carboxylic acid (9c).

M.P.: 238–240; yield: 62%; IR (KBr) v_{max}: 3500 (OH), 3379 (NH), 3008 (C–H arom.), 2912 (C–H aliph.), 1712 (C=O) cm^{-1}; ^{1}H NMR (DMSO-d$_6$): δ 1.17–1.20 (m, 2H, CH$_2$ cyclo-propyl), 1.33–1.35 (m, 2H, CH$_2$ cyclopropyl), 3.40 (s, 2H, CH$_2$CO), 3.49–3.50 (m, 4H, 2CH$_2$ piperazine), 3.75 (s, 3H, CH$_3$O), 3.83–3.84 (m, 1H, CH cyclopropyl), 4.14–4.15 (m, 4H, 2CH$_2$ piperazine), 6.82 (d, 2H, $J = 8.0$ Hz, ArH), 7.19 (d, 2H, $J = 8.0$ Hz, ArH), 7.59 (d, 1H, $J = 8.0$ Hz, ArH), 7.90 (d, 1H, $J = 13.20$ Hz, ArH), 8.67 (s, 1H, C2-H), 9.34 (s, 2H, 2NH, D$_2$O exchangeable) and 15.16 (s, 1H, COOH, D$_2$O exchangeable); ^{13}C NMR (DMSO-d$_6$): δ 8.0, 36.3, 40.4, 47.7, 49.1, 55.6, 106.5, 107.1, 111.3, 111.5, 113.7, 118.8, 118.9, 127.8, 134.1, 145.1, 148.4, 151.9, 157.0, 166.5, 176.7, 182.2 ppm. Anal. Calcd. for $C_{27}H_{29}FN_6O_5S$ (568.62): C, 57.03; H, 5.14; N, 14.78. Found: C, 57.21; H, 5.38; N, 15.02.

General procedure for the preparation of 1-cyclopropyl-6-fluoro-7-(4-((N'-2-(substituted phenyl)-2-oxoethyl)hydrazine carbonyl)me-thyl)piperazin-1-yl)-4-oxo-1,4-dihydroquinoline-3-carboxylic acid (10a–c)

A mixture of hydrazinyl derivative **2** (0.50 g, 0.001 mol), anhydrous potassium carbonate (0.41 g, 0.003 mol) and substituted phenacyl bromide (0.001 mol) in dry benzene (8 ml) was heated under reflux for 24 h. The reaction mixture was filtered while hot. The residue was washed twice with water (20 ml), dried, and recrystallised from ethanol to give compound **10a–c**.

1-Cyclopropyl-6-fluoro-4-oxo-7-(4-(2-oxo-2-(2-(2-oxo-2-phenyl-eth-yl)hydrazinyl)ethyl) piperazin-1-yl)-1,4-dihydroquinoline-3-carbox-ylic acid (10a).

M.P.: 183–185 °C; yield: 45%; (KBr) v_{max}: 3500 (OH), 3402 (NH), 3008 (C–H arom.), 2916 (C–H aliph.), 1732, 1700, 1697 (C=O) cm^{-1}; ^{1}H NMR (DMSO-d$_6$): δ 1.11–1.18 (m, 2H, CH$_2$ cyclo-propyl), 1.30–1.32 (m, 2H, CH$_2$ cyclopropyl), 2.75–2.79 (m, 2H, CH$_2$ piperazine), 2.90–2.95 (m, 2H, CH$_2$ piperazine), 3.40 (s, 2H,CH$_2$CO), 3.45–3.50 (m, 2H, CH$_2$ piperazine), 3.60–3.70 (m, 2H, CH$_2$ pipera-zine), 3.80–3.90 (m, 1H, CH cyclopropyl), 4.00 (s, 2H, CH$_2$CO), 5.61 (s, 1H, NH, D$_2$O exchangeable), 7.37–8.05 (m, 7H, ArH), 8.56 (s, 1H, C2-H), 8.66 (s, 1H, NH, D$_2$O exchangeable), ppm; ^{13}C NMR (DMSO-d$_6$): δ 7.9, 17.0, 26.0, 36.5, 46.2, 50.0, 102.0, 111.0, 116.5, 126.0, 127.4, 128.5, 129.4, 143.0, 144.5, 150.5, 161.0, 166.6, 174.5 ppm. Anal. Calcd. for $C_{27}H_{28}FN_5O_5$ (521.54): C, 62.18; H, 5.41; N, 13.43. Found: C, 61.96; H, 4.70; N, 13.72.

7-(4-(2-(2-(2-(3-Bromophenyl)-2-oxoethyl)hydrazinyl)-2-oxo-ethyl)-piperazin-1-yl)-1-cyclopropyl-6-fluoro-4-oxo-1,4-dihydroquinoline-3-carboxylic acid (10b).

M.P.: 210–215 °C; yield: 62%; IR (KBr) v_{max}: 3500 (OH), 3240 (NH), 3020 (C–H arom.), 2920 (C–H aliph.), 1725 (C=O) cm^{-1}; ^{1}H NMR (DMSO-d$_6$): δ 1.16–1.18 (m, 2H, CH$_2$ cyclo-propyl), 1.29–1.32 (m, 2H, CH$_2$ cyclopropyl), 2.90–3.00 (m, 4H, 2CH$_2$ piperazine), 3.22–3.24 (m, 4H, 2CH$_2$ piperazine), 3.30 (s, 2H, CH$_2$CO), 3.40–3.70 (m, 3H, CH cyclopropyl, CH$_2$CO), 7.35–7.40 (m, 1H, ArH), 7.40–7.48 (m, 1H, ArH), 7.50 (d, 1H, $J = 8$ Hz, ArH), 7.81 (m, 5H, 3ArH, 2NH), and 8.62 (s, 1H, C2-H) ppm; ^{13}C NMR (DMSO-d$_6$): δ 8.0, 27.0, 36.2, 45.40, 50.6, 53.0, 106.5, 107.1, 111.1, 111.4, 118.7, 123.7, 124.3, 128.7, 129.3, 135.7, 139.6, 146.0, 148.2, 152.1, 154.6, 166.4, 167.2, 176.7 ppm. Anal. Calcd. for $C_{27}H_{27}BrFN_5O_5$ (600.45): C, 54.01; H, 4.53; N, 11.66. Found: C, 55.21; H, 4.82; N, 12.03.

1-Cyclopropyl-6-fluoro-7-(4-(2-(2-(2-(4-nitrophenyl)-2-oxoethyl)-hydrazinyl)-2-oxoethyl)piperazin-1-yl)-4-oxo-1,4-dihydroquinoline-3-carboxylic acid (10c).

M.P.: 221–223 °C; yield: 55%; IR (KBr) v_{max}: 3540 (OH), 3402 (NH), 3008 (C–H arom.), 2950 (C–H aliph.), 1730 (C=O) cm^{-1}; ^{1}H NMR (DMSO-d$_6$): δ 1.10–1.15 (m, 2H, CH$_2$ cyclo-propyl), 1.30–1.35 (m, 2H, CH$_2$ cyclopropyl), 2.80–2.85 (m, 4H, 2CH$_2$ piperazine), 3.20–3.25 (m, 4H, 2CH$_2$ piperazine), 3.30 (s, 2H, CH$_2$CO), 3.60 (s, 2H, CH$_2$CO), 3.80–3.90 (m, 1H, CH cyclopropyl), 7.36 (s, 1H, NH, D$_2$O exchangeable), 7.50–7.60 (m, 2H, ArH), 7.70 (d, 1H, ArH), 8.10–8.50 (m, 3H, ArH), 8.59 (s, 1H, NH, D$_2$O exchangeable), and 8.66 (s, 1H, C2-H) ppm; ^{13}C NMR (DMSO-d$_6$): δ 8.0, 29.0, 31.5, 36.0, 45.5, 50.8, 106.5, 108.6, 111.2, 111.4, 119.3, 121.2, 128.2, 129.8, 131.4, 132.2, 139.5, 148.1, 152.1, 154.6, 166.6, 176.4 ppm. Anal. Calcd. for $C_{27}H_{27}FN_6O_7$ (566.55): C, 57.24; H, 4.80; N, 14.83. Found: C, 57.41; H, 4.98; N, 15.09.

Procedure for the preparation of 1-cyclopropyl-7-(4-(2-((2,5-dioxo-pyrrolidin-1-yl)amino)-2-oxoethyl)piperazin-1-yl)-6-fluoro-4-oxo-1,4-dihydroquinoline-3-carboxylic acid (11).

A mixture of hydra-zinyl derivative **2** (0.50 g, 0.001 mol), succinic anhydride (0.10 g, 0.001 mol), and anhydrous sodium acetate (0.117 g, 0.0015 ml) in glacial acetic acid (10 ml) was heated under reflux for 5 h. The reaction mixture was concentrated to half its volume and allowed to cool, the separated solid was filtered, washed with cold etha-nol, dried, and recrystallised from acetic acid to give compound **11**. M.P.: 184–186 °C; yield: 55%; IR (KBr) v_{max}: 3441 (OH), 3224 (NH), 3016 (C–H arom.), 2947 (C–H aliph.), 1720, 1712, 1700 (C=O) cm^{-1}; ^{1}H NMR (DMSO-d$_6$): δ 1.18–1.20 (m, 2H, CH$_2$ cyclo-propyl), 1.31–1.33 (m, 2H, CH$_2$ cyclopropyl), 2.24 (s, 4H, 2CH$_2$ pyr-rolidine), 2.70–2.80 (m, 4H, 2CH$_2$ piperazine), 3.10 (s, 2H, CH$_2$CO), 3.30–3.40 (m, 4H, 2CH$_2$ piperazine), 3.83–3.84 (m, 1H, CH cyclo-propyl), 7.56 (d, 1H, $J = 8$ Hz, ArH), 7.90 (d, 1H, $J = 13.6$ Hz, ArH), 8.66 (s, 1H, C2-H), and 9.68 (s, 1H, NH, D$_2$O exchangeable) ppm. ^{13}C NMR (DMSO-d$_6$): δ 8.0, 19.5, 20.8, 26.6, 28.7, 29.8, 106.6, 107.3, 111.2, 111.4, 119.0, 139.5, 145.5, 148.2, 152.1, 154.6, 168.4, 176.6 ppm. $C_{23}H_{24}FN_5O_6$ (485.46): C, 56.90; H, 4.98; N, 14.43. Found: C, 56.87; H, 4.95; N, 14.41.

Procedure for the preparation of 1-cyclopropyl-7-(4-(2-((1,3-dioxoi-soindolin-2-yl)amino)-2-oxoethyl)piperazin-1-yl)-6-fluoro-4-oxo-1,4-dihydroquinoline-3-carboxylic acid (12).

A mixture of compound **2** (0.50 g, 0.001 mol), phthalic anhydride (0.15 g, 0.001 mol), and anhydrous sodium acetate (0.117 g, 0.0015 ml) in glacial acetic acid (10 ml) was heated under reflux for 5 h. The reaction mixture was concentrated to half its volume and allowed to cool, the sep-arated solid was filtered, washed with cold ethanol, dried, and

recrystallised from acetic acid to give compound **12**. M.P: 190–192 °C; yield: 50%; IR (KBr) v_{max}: 3441 (OH), 3224 (NH), 3012 (C–H arom.), 2897 (C–H aliph.), 1720, 1700 (C=O) cm^{-1}; ^{1}H NMR (DMSO-d$_6$): δ 1.10–1.15 (m, 2H, CH$_2$ cyclopropyl), 1.20–1.30 (m, 2H, CH$_2$ cyclopropyl), 2.65–2.75 (m, 4H, 2CH$_2$ piperazine), 3.11 (s, 2H, CH$_2$CO), 3.25–3.35 (m, 4H, 2CH$_2$ piperazine), 3.75–3.80 (m, 1H, CH cyclopropyl), 7.36–8.15 (m, 6H, ArH), 8.63 (s, 1H, C2-H), and 9.74 (s, 1H, NH, D$_2$O exchangeable) ppm. Anal. Calcd. for C$_{27}$H$_{24}$FN$_5$O$_6$ (533.51): C, 60.78; H, 4.53; N, 13.13. Found: C, 60.92; H, 4.58; N, 13.11.

Procedure for the preparation of 7-(4-(2-(2-carbamothioylhydrazinyl)-2-oxoethyl) piperazin-1-yl)-1-cyclopropyl-6-fluoro-4-oxo-1,4-dihydroquinoline-3-carboxylic acid (13).

A mixture of hydrazinyl derivative **2** (0.50 g, 0.001 mol), potassium thiocyanate (0.194 g, 0.002 mol), and concentrated hydrochloric acid (1 ml) in absolute ethanol (15 ml) was heated under reflux for 6 h. The reaction mixture was cooled, and the separated solid was filtered, dried, and recrystallised from ethanol to give compound **13**. M.P.: 188–200 °C; yield: 65%; IR (KBr) v_{max}: 3417 (OH), 3271, 3236 (NH, NH$_2$), 3001 (C–H arom.), 2947 (C–H aliph.), 1747, 1728 (C=O) cm^{-1}; ^{1}H NMR (DMSO-d$_6$): δ 1.19–1.21 (m, 2H, CH$_2$ cyclopropyl), 1.34–1.35 (m, 2H, CH$_2$ cyclopropyl), 3.30–3.50 (m, 8H, 4CH$_2$ piperazine), 3.67 (s, 2H, CH$_2$CO), 3.87–3.89 (m, 1H, CH cyclopropyl), 7.20 (s, 1H, NH, D$_2$O exchangeable), 7.30 (s, 2H, NH$_2$, D$_2$O exchangeable), 7.40 (s, 1H, NH, D$_2$O exchangeable), 7.63 (d, 1H, $J = 8$ Hz, ArH), 7.96 (d, 1H, $J = 13$ Hz, ArH), 8.68 (s, 1H, C2-H), and 15.20 (s, 1H, COOH, D$_2$O exchangeable) ppm; ^{13}C NMR (DMSO-d$_6$): δ 8.0, 14.5, 17.0, 51.8, 56.1, 107.2, 130.0, 144.3, 148.4, 148.5, 152.0, 152.1, 154.5, 166.2, 166.3, 168.5, 176.7 ppm. Anal. Calcd. for C$_{20}$H$_{23}$FN$_6$O$_4$S (462.5): C, 51.94; H, 5.01; N, 18.17 Found: C, 51.91; H, 5.12; N, 18.22

Procedure for the preparation of 1-cyclopropyl-6-fluoro-4-oxo-7-(4-(2-oxo-2-(2-(4-oxothiazolidin-2-ylidene)hydrazinyl)ethyl)piperazin-1-yl)-1,4-dihydroquinoline-3-carboxylic acid (14).

A mixture of compound **13** (0.23 g, 0.0005 mol), ethyl chloroacetate (0.60 g, 0.005 mol) in absolute ethanol (15 ml) was heated under reflux for 6 h. The obtained precipitate was filtered, washed with water, dried, and recrystallised from ethanol to form compound **14**. MP: 240–242 °C; yield: 70%; IR (KBr) v_{max}: 3417 (OH), 3271 (NH), 3020 (C–H arom.) 2947(C–H aliph.), 1720 (C=O) cm^{-1}; ^{1}H NMR (DMSO-d$_6$): δ 1.18–1.20 (m, 2H, CH$_2$ cyclopropyl), 1.34–1.36 (m, 2H, CH$_2$ cyclopropyl), 2.60–2.80 (m, 4H, 2CH$_2$ piperazine), 3.28 (s, 4H, 2CH$_2$CO), 3.30–3.35 (m, 4H, 2CH$_2$ piperazine), 3.51 (brs, 2H, 2NH, D$_2$O exchangeable), 3.80–3.90 (m, 1H, CH cyclopropyl), 7.58 (d, 1H, $J = 8.0$ Hz, ArH), 7.90 (d, 1H, $J = 13$ Hz, ArH), 8.66 (s, 1H, C2-H), and 15.21 (s, 1H, COOH, D$_2$O exchangeable) ppm. ^{13}C NMR (DMSO-d$_6$): δ 6.2, 21.4, 29.3, 44.6, 52.6, 60.5, 106.4, 111.2, 114.5, 121.0, 144.5, 144.6, 156.0, 165.5, 170.2, 178.1, 188.2 ppm. Anal. Calcd. for C$_{22}$H$_{23}$FN$_6$O$_5$S (502.52): C, 52.58; H, 4.61; N, 16.72. Found: C, 52.79; H, 4.75; N, 16.88.

Procedure for the preparation of 1-cyclopropyl-6-fluoro-4-oxo-7-(4-(2-oxo-2-(2-(4-phenylthiazol-2(3H)-ylidene)hydrazinyl)ethyl)piperazin-1-yl)-1,4-dihydroquinoline-3-carboxylic acid (15).

A mixture of compound **13** (0.18 g, 0.0004 mol), phenacyl bromide (0.08 g, 0.0004 mol), and anhydrous sodium acetate (0.03 g, 0.0004 mol) in absolute ethanol (15 ml) was heated under reflux for 6 h. The obtained precipitate was filtered, washed with water, dried, and recrystallised from ethanol to form compound **15**. M.P.: 256–258 °C; yield: 25%; IR (KBr) v_{max}: 3549 (OH), 3317 (NH), 3089

(C–H arom.) 2912 (C–H aliph.), 1728 (C=O) cm^{-1}; ^{1}H NMR (DMSO-d$_6$): δ 1.19–1.20 (m, 2H, CH$_2$ cyclopropyl), 1.33–1.35 (m, 2H, CH$_2$ cyclopropyl), 2.21–2.23 (m, 4H, 2CH$_2$ piperazine), 3.36–3.38 (m, 4H, CH$_2$CO and 2NH), 3.70–3.75 (m, 4H, 2CH$_2$ piperazine), 3.80–3.90 (m, 1H, CH cyclopropyl), 7.15–7.20 (m, 3H, ArH), 7.35 (d, 2H, ArH), 7.55 (d, 1H, $J = 8.0$ Hz, ArH), 7.85 (d, 1H, $J = 13.0$ Hz, ArH), 8.31 (s, 1H, thiazole-H), 8.62 (s, 1H, C2-H), and 14.80 (s, 1H, COOH, D$_2$O exchangeable) ppm. ^{13}C NMR (DMSO-d$_6$): δ 8.0, 18.8, 36.3, 44.2, 49.9, 106.9, 107.1, 111.5, 119.1, 119.2, 127.2, 127.7, 129.3, 133.2, 135.6, 139.3, 145.5, 148.3, 152.1, 154.6, 155.7, 166.3, 176.7 ppm. Anal. Calcd. for C$_{28}$H$_{27}$FN$_6$O$_4$S (562.18): C, 59.78; H, 4.84; N, 14.94. Found: C, 59.50; H, 5.22; N, 14.84.

Biological activity

Cell culture protocol

Human bladder cancer (T-24) and human prostate carcinoma (PC-3) cell lines were obtained from American Type Culture Collection (ATCC; Manassas, VA USA). Cells were maintained in Dulbecco's modified Eagle medium with 10% foetal bovine serum at 37 °C and 5% CO$_2$. All the operations were carried out under strict aseptic conditions. The culture medium was removed to a centrifuge tube containing 9.0 ml complete culture medium and spanned at approximately 125 × g for 5 to 7 min. The cell layer was rinsed with 0.25% (w/v) trypsin- 0.53 μM EDTA solution by which all traces of serum-containing inhibitor were removed. Trypsin EDTA solution 2.0 to 3.0 ml was added to a flask and cells were monitored under an inverted microscope until the cell layer was dispersed (usually within 5–15 min). A complete growth medium was added (6.0–8.0 ml), and cells were aspirated by gentle pipetting. The cell pellet was suspended with the recommended complete medium and dispensed into a 75 cm^2 culture flask. The culture vessel containing the complete growth medium was placed in the incubator for 24 h to at 37 °C. The cells were treated with different concentrations (0.39, 1.60, 6.25, 25, and 100 μg/ml) of each of the test compounds or doxorubicin, followed by incubation for 48 h at 37 °C, then the plates were examined under the inverted microscope and finally the MTT assay was carried out.

Cell viability assay

Anti-cancer activity of the newly synthesised compounds was evaluated in vitro against both T-24 and PC-3 cell lines according to the MTT method[62]. Cells were seeded into 96-well plates (flat bottom) at a density of 10 000 cells/well for 24 h. The vial of MTT to be used was reconstituted with 3 ml of medium or balanced salt solution without phenol red and serum. then, a reconstituted MTT vial was added in an amount equal to 10% of the culture medium volume. Cultures were incubated for 2–4 h depending on the cell type and maximum cell density and removed from the incubator and the formazan crystals were dissolved via the addition of an amount of MTT solubilisation solution (M-8910) equal to the original culture medium volume. ROBONIK P2000 spectrophotometer at a wavelength of 570 nm was used to measure the colour intensity spectrophotometrically. The survival curve of both T-24 and PC-3 cells was obtained by plotting the percentage of surviving cells against the drug after each compound. The IC$_{50}$ value for each test compound and the reference drug doxorubicin was calculated.

In vitro DNA topo II-mediated relaxation assay

DNA Topo II inhibitory activities of the targeted compounds were measured as follows. A mixture of 100 ng of supercoiled pBR322 plasmid DNA (Fermentas, USA) and 2 units of human DNA Topo II (USB Corp., USA) was incubated with and without the prepared compounds in the assay buffer (10 µM Tris-HCl pH 7.9) containing 50 µM NaCl, 4 µM $MgCl_2$, 1 µM EDTA, 1 µM ATP, and 15 mg/ml bovine serum albumin for 30 min at 37 °C. The reaction in a final volume of 10 µl was terminated by the addition of 4 µl of 6 µM EDTA. DNA samples were then electrophoresed on 1% agarose gel containing 0.5 µg/ml ethidium bromide in gel and buffer at high voltage (100–250 v) until the dye front has migrated about 4–6 cm down the gel. with a running buffer of TAE Tris-acetate–EDTA (TAE). Gels were stained for 15 min in water. DNA bands were visualised by transillumination with UV light and quantitated using AlphaI-maker TM (Alpha Innotech Corporation).

Cell cycle analysis of compounds 6 and 8a

The cell cycle was done using a propidium iodide flow cytometry kit (Abcam, ab139418) according to the manufacturer's instructions. T-24 and PC-3 cells were treated with IC_{50} of compounds **6** and **8a** for 24 h. After treatment, the cells were washed twice with ice-cold phosphate buffer saline, then centrifuged and fixed using ice-cold 66% (v/v) ethanol, washed with phosphate buffer saline re-suspended with 0.10 mg/ml, and stained with 200 µl propidium iodide. Cells were analysed by flow cytometry. The cell cycle distributions were calculated using cell–quest software (Bectopn Dickinson).

Apoptosis determination

Apoptosis was evaluated using Annexin V fluorescein isothiocyanate (FITC) and propidium iodide (PI) using the Annexin V-FITC/PI apoptosis detection kit (Biovision, Mountain View, CA # K101-25). According to the manufacturer's instructions after staining the cells with annexin V fluorescein (FITC) isothiocyanate. Briefly, $1–5 \times 10^5$ cells were exposed to compounds **6** and **8a** at their IC_{50} concentrations for 24 h. Cells were centrifuged and washed once with serum-containing media followed by resuspension in 500 µl of binding buffer. Then 5 µl Annexin V-FITC and 5 µl of (PI 50 mg/ml) were added and incubated for 5 min at room temperature in the dark. Analyses were performed using a flow cytometer (EX = 488 nm: Em = 530 nm) using a FITC signal detector and PI staining by a phycoerythrin emission signal detector.

Measurement of the effect of compounds 6 and 8a on the level of caspase-3 protein (a marker of apoptosis)

The level of the apoptotic marker caspase-3 was measured using The Invitrogen Caspase-3 (active) Human ELISA Kit. The procedure of the used kit was done according to the manufacturer's instructions.

Molecular docking study

Molecular docking studies were performed using the Molecular Operating Environment (MOE, 2014.0901) software. All minimisations were performed using MOE with MMFF94x force field, and the partial and formal charges were calculated automatically. The X-ray crystallographic structures of topoisomerase IIα co-crystallised with DNA[63] were downloaded from the protein data bank[64]. To prepare the enzyme for the docking study, first DNA chains and water molecules were removed, and then the protonate 3D protocol in MOE with default options was used. For the docking protocol, the triangle matcher placement method and London dG scoring function were used. Validation of the docking results was carried out by docking the reference topoisomerase inhibitor merbarone and comparing the results with a previously reported study. The MOE-validated setup was used to predict the binding interactions and affinity of the synthesised compounds at the active site.

Results and discussion

Chemistry

The synthetic approaches designed in this study for the synthesis of the target compounds are elucidated in Schemes 1–3. The primary starting compound **1**, was prepared by reacting CP with ethyl chloroacetate in dimethylformamide in the presence of trimethylamine[39]. Compound **1** was reacted with hydrazine hydrate to afford compound **2**[39].

Compound **3** was prepared by reacting hydrazinyl derivative **2** with ethyl acetoacetate in absolute ethanol. The ^1H NMR spectrum of this compound displayed the disappearance of the signal corresponding to NH_2 of the parent compound **2** and the appearance of two singlet signals at δ 2.47 and 3.80 ppm corresponding to $CH_3C=N$ and CH_2 pyrazolone protons, respectively.

CP derivative **4** was prepared by reacting compound **2** with ethyl cyanoacetate in glacial acetic acid, the ^1H NMR spectrum displayed a singlet signal at δ 3.86 ppm expressing the CH_2 pyrazolone protons. Compound **5** was obtained via refluxing CP hydrazinyl derivative **2** with acetylacetone in ethanol. The ^1H NMR spectrum displayed the disappearance of the signal corresponding to NH_2 of the parent compound **2** in addition to the presence of one singlet signal at δ 7.90 ppm corresponding to CH of pyrazole.

Compound **6** was obtained by reacting compound **2** with diethyl malonate in the presence of sodium ethoxide. The ^1H NMR spectrum of this compound revealed the appearance of a singlet signal at δ 2.90 ppm due to the CH_2 of pyrazolone.

In Scheme 2, the hydrazones **7a–f** were obtained by reacting compound **2** with the appropriate ketone in ethanol in the presence of glacial acetic acid. The ^1H NMR and ^{13}C NMR spectra of these compounds displayed the presence of signals corresponding to different alkyl or aryl groups which were not present in compound **2**.

Refluxing compound **2** with the suitable isatin in absolute ethanol in the presence of glacial acetic acid afforded compounds **8a–b**. The ^1H NMR and ^{13}C NMR spectra of these compounds revealed the presence of different signals of indoline moieties.

Compounds **9a–c** were prepared via reacting compound **2** with the appropriate phenyl isocyanates or phenyl isothiocyanate in absolute ethanol in the presence of glacial acetic acid. The ^1H NMR and ^{13}C NMR spectra of these derivatives displayed the characteristic signals corresponding to different aryl moieties. Further structural evidence stemmed from the ^1H NMR spectra that showed the exchangeable singlet signals corresponding to NH protons.

CP derivatives **10a–c** were prepared via reacting compound **2** with the suitable phenacyl bromide in dry benzene in the presence of potassium carbonate. The ^1H NMR and ^{13}C NMR spectra of these derivatives showed the appearance of new signals corresponding to the added phenyl ring in addition to singlet signals that appeared at δ 3.30–3.40 ppm due to CH_2CO protons.

In Scheme 3, the reaction of compound **2** with succinic anhydride or phthalic anhydride in glacial acetic acid in the presence of anhydrous sodium acetate yielded compounds **11** and **12**,
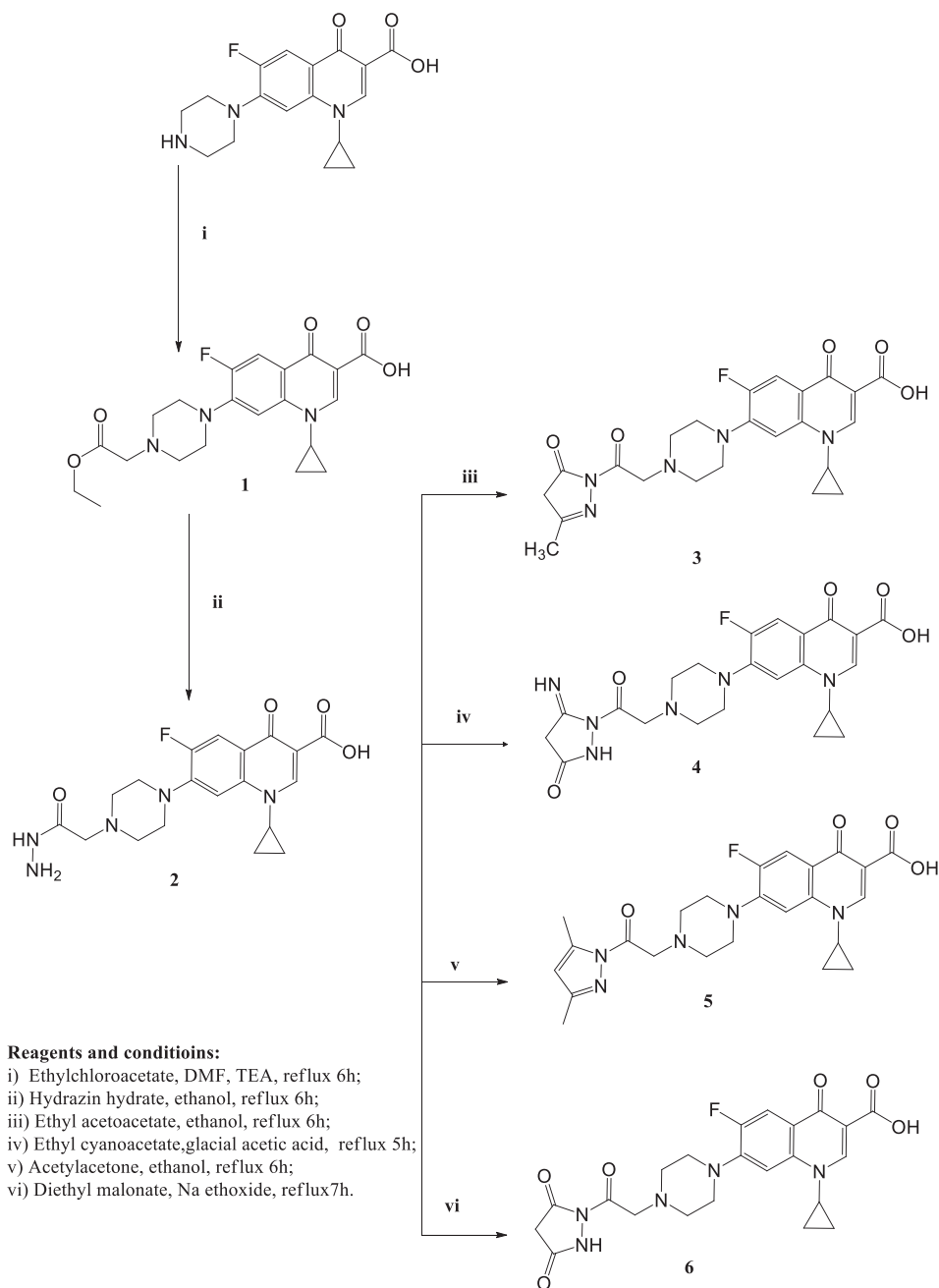
Scheme 1. The synthetic path and reagents for the preparation of the target compounds 1–6.

Reagents and conditioins:
i) Ethylchloroacetate, DMF, TEA, reflux 6h;
ii) Hydrazin hydrate, ethanol, reflux 6h;
iii) Ethyl acetoacetate, ethanol, reflux 6h;
iv) Ethyl cyanoacetate,glacial acetic acid, reflux 5h;
v) Acetylacetone, ethanol, reflux 6h;
vi) Diethyl malonate, Na ethoxide, reflux7h.

respectively. The ^{1}H NMR and ^{13}C NMR spectra of these compounds showed the appearance of new signals corresponding to pyrrolidine and isoindoline moieties.

Reacting compound **2** with potassium thiocyanate and concentrated hydrochloric acid in absolute ethanol afforded compound **13**. ^{13}C NMR spectrum revealed the appearance of (C = S) carbon at δ 176.7 ppm. Compound **14** was prepared via reacting derivative **13** with ethyl chloroacetate in ethanol. The ^{1}H NMR spectrum of compound **14** revealed the disappearance of the exchangeable signal of NH$_2$ protons.

Finally, compound **15** was prepared by refluxing compound **13** with phenacyl bromide in absolute ethanol in the presence of anhydrous sodium acetate. The ^{1}H NMR and ^{13}C NMR spectra showed the expected signals corresponding to the phenyl group, which were not present in the starting compound **14**. Additionally, the ^{1}H NMR spectrum revealed the appearance of a

single signal corresponding to CH of the thiazole ring at δ 8.31 ppm.

Biological activity

Growth inhibition against human tumour cell lines

In this study, all the newly synthesised CP derivatives were subjected to anticancer activity evaluation against bladder (T-24) and prostate cancer (PC-3) cell lines. The compounds were evaluated for their activity using 5 doses determinations (100 μg/ml, 25 μg/ml, 6.25 μg/ml, 1.60 μg/ml, and 0.39 μg/ml). Their half-maximal inhibitory concentration (IC$_{50}$) values were measured. Doxorubicin was chosen as a reference anticancer drug[65].

The test compounds showed anticancer activity against the T-24 cell line with IC$_{50}$ values ranging from 3.36–366 μM. They
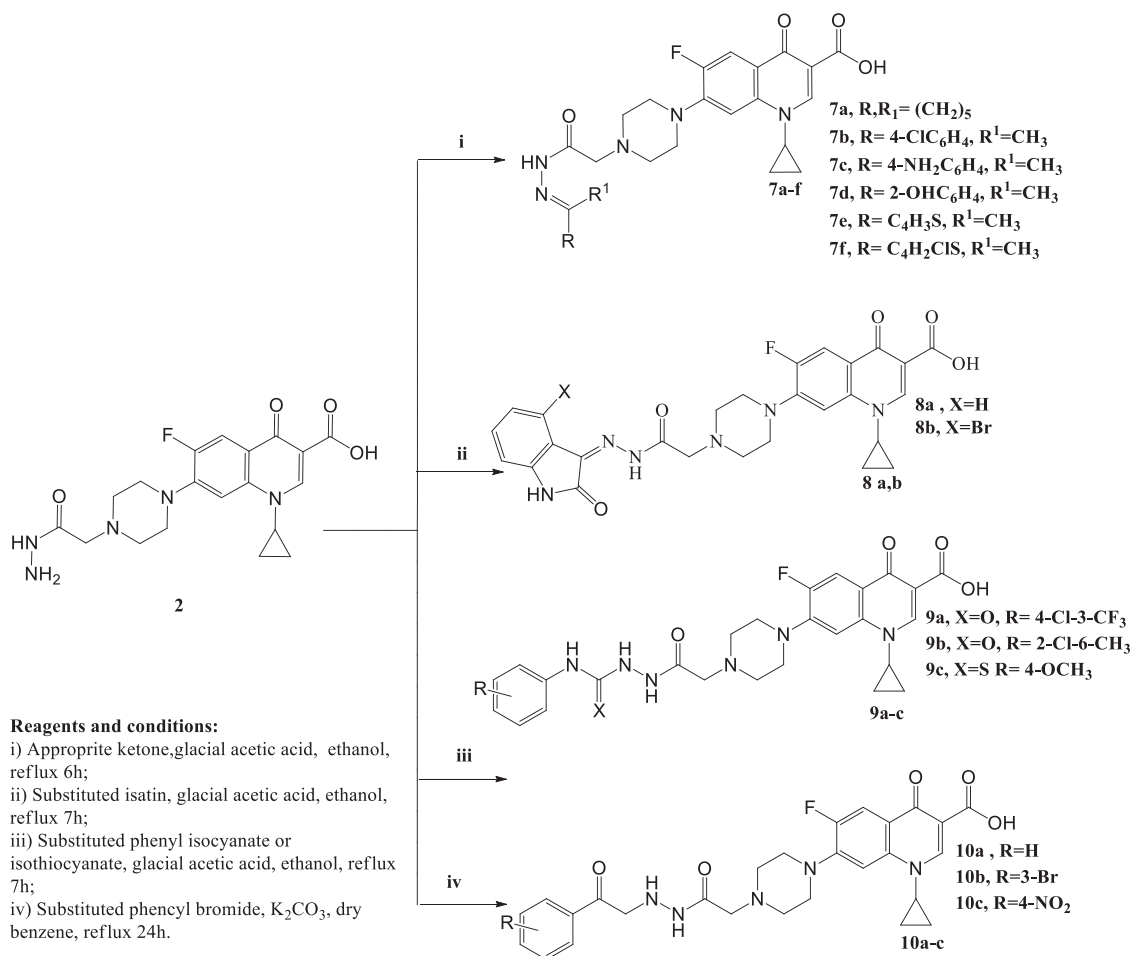
Scheme 2. The synthetic path and reagents for the preparation of the target compounds **7–10**.

exhibited IC$_{50}$ values against the PC-3 cell line in the range of 3.25–159.24 μM (Table 1).

Compounds **4–6**, **7a–c**, **7e**, **8a**, **9a–b**, **10b–c**, **14**, and **15** showed 1.02- to 8.66-fold more potent anti-proliferative activity than the reference standard doxorubicin against T-24 cell line (Figure 4).

Compounds **7a–b**, **7d**, **8a**, **9b–c**, **10b–c**, **14**, and **15** exhibited 1.2- to 7.1-fold more potent anti-proliferative activity than doxorubicin against PC-3 cells line (Figure 5).

Regarding the activity towards bladder cancer, compounds **6**, **7a**, **7b**, **8a**, **9a**, and **10c** were the most potent among the synthesised CP derivatives.

It is worth mentioning that the T-24 bladder cancer cell line was more sensitive to the synthesised CP derivatives than the PC-3 prostate cancer cell line.

The Structure-activity correlation of the newly synthesised CP derivatives revealed that modification at the piperazinyl N-4 position of the CP scaffold resulted in variable potency. CP derivatives bearing pyrazole ring through acetyl spacer (**4–6**) showed potent anticancer activity. They showed more potency against bladder cancer cell line, compound **6** incorporating pyrazolidine-3,5-dione moiety was the most prominent among them. Regarding CP hydrazones **7a–e**, compound **7a** incorporating cyclohexylidene moiety showed marked potency against bladder and prostate cancer cell lines. Further analysis of these compounds revealed that hydrazones carrying substituted phenyl ring (**7b–d**) were more potent than their counterparts having thiophene ring (**7e,f**). An interesting phenomenon is that CP hydrazone **7d** featuring ortho

hydroxyl group on the phenyl ring showed the most potent anti-proliferative activity among CP aryl hydrazones against prostate cancer. CP derivative **8a** having the acylhydrazone scaffold with a benzene ring carrying a nearby NH proved to marked anti-proliferative activity against both cell lines. It was clear that the introduction of a bromine atom on the indoline scaffold (**8b**) had a bad impact on the anticancer activity. CP semicarbazide and thiosemicarbazide derivatives **9a–c** possessed potent activity. It was noticed that compound **9a** featuring the 4-chloro-3-trifluoromethylphenyl moiety group was the most potent. Reviewing compounds **10a–c**, revealed that the substitution of phenyl moiety with electron withdrawing group in **10b** and **10c** significantly improved the anticancer activity against the two cell lines. The incorporation of monocyclic pyrrolidine or pyrrolidine fused with benzene in CP derivatives **11** and **12** resulted in lower anticancer activity. It is worth mentioning that, grafting thiazole moiety in derivatives **14** and **15** highly improved the antiproliferative activity.

Recombinant topoisomerase II inhibitory activities of compounds (6, 7a, 7b, 8a, 9a, and 10c)

The conversion of supercoiled plasmid DNA to relaxed DNA by recombinant Topo II was examined in the presence of each of the most potent compounds **6**, **7a**, **7b**, **8a**, **9a**, and **10c** for measuring their Topo II inhibitory activities. Well-known Topo II inhibitor doxorubicin was used as a positive control. The reaction products of Topo II relaxation assays were analysed by electrophoretic
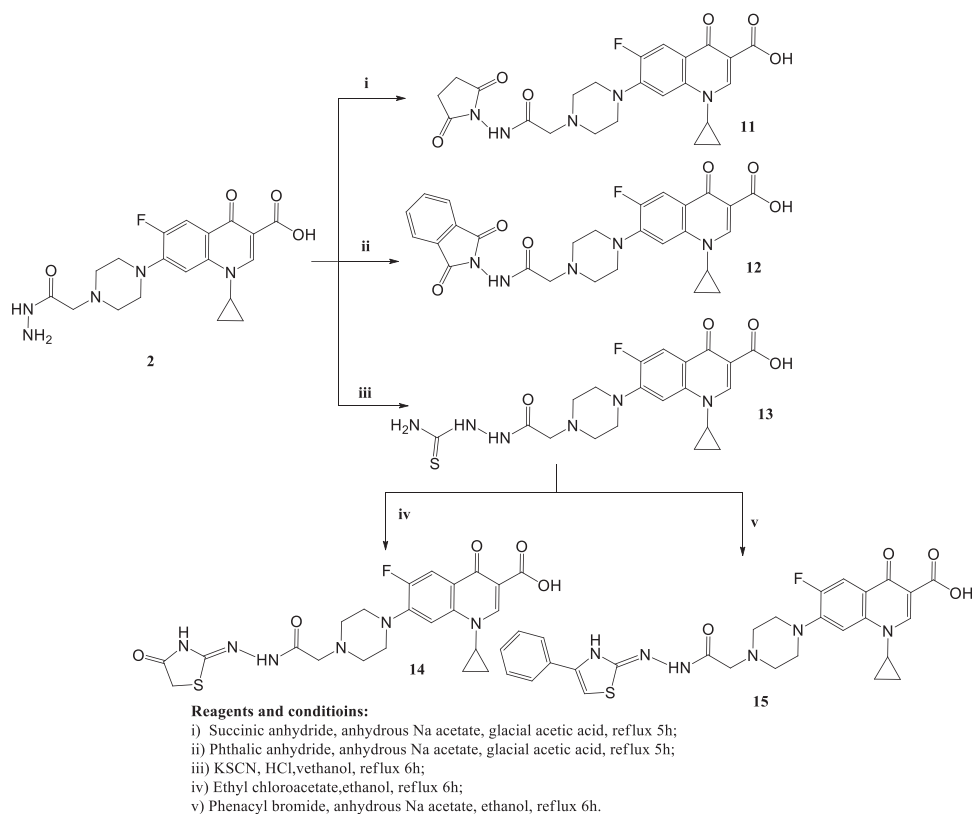
Scheme 3. The synthetic path and reagents for the preparation of the target compounds **11–15**.

Table 1. The half-maximal inhibitory concentration (IC$_{50}$) of CP derivatives and doxorubicin after treatment for 24 h on both the prostate cancer cell line (PC-3) and bladder cancer cell line (T-24).

Compound	IC$_{50}$ (µM* ± SD)	
	T-24	PC-3
3	37.32 ± 2.02	98.20 ± 5.00
4	**25.46 ± 1.38**	29.89 ± 1.53
5	**25.90 ± 1.39**	24.94 ± 1.26
6	**5.68 ± 0.3**	92.16 ± 4.69
7a	**3.88 ± 0.21**	**9.35 ± 0.48**
7b	**11.50 ± 0.63**	**19.04 ± 0.96**
7c	**25.59 ± 0.71**	32.77 ± 0.86
7d	88.02 ± 4.75	**8.81 ± 0.44**
7e	**25.00 ± 0.2**	50.49 ± 10.36
7f	124.27 ± 6.7	136.26 ± 6.94
8a	**3.36 ± 0.19**	**10.95 ± 0.56**
8b	336.10 ± 18.15	41.05 ± 2.09
9a	**4.35 ± 0.24**	67.17 ± 3.42
9b	**28.55 ± 1.54**	**19.33 ± 0.98**
9c	134.01 ± 7.23	**4.85 ± 0.27**
10a	45.44 ± 2.45	74.31 ± 3.78
10b	**17.23 ± 0.93**	**3.38 ± 0.18**
10c	**10.08 ± 0.55**	**3.25 ± 0.167**
11	68.47 ± 3.69	82.21 ± 4.18
12	47.00 ± 1.09	125.58 ± 6.39
13	34.51 ± 1.86	30.53 ± 1.56
14	**19.48 ± 0.58**	**6.49 ± 0.24**
15	**15.92 ± 0.87**	**7.54 ± 0.39**
Doxorubicin	29.11 ± 1.56	23.07 ± 1.18

*The results given are the means of three experiments.
Bold values indicate that these CP derivatives are more potent than Doxorubicin.

mobility and developed in ethidium bromide in the presence of UV light. The inhibitory activities were evaluated at 4 concentrations of 100, 10, 1, and 0.1 µM for all compounds as shown in (Figure 6). Topo II inhibitory activities of the tested compounds are summarised in (Table 2).

All test compounds showed significant Topo II inhibitory activity in the range of 83–90% at 100 µM concentration. While at 0.1 µM concentration, the range of Topo II inhibition was 13.7–32.5% (Table 2). The IC$_{50}$ value of each compound was calculated. Compounds **6**, **8a**, and **10c** were 1.01- to 2.32-fold more potent than doxorubicin (Table 3).

Cell cycle analysis and detection of apoptosis

The most prominent compounds **6** and **8a** that showed Topo II IC$_{50}$ values in the sub-micro-molar range were further investigated in terms of their effects on apoptosis induction and cell cycle progression in both T-24 and PC-3 cell lines.

T-24 and PC-3 cells were treated with compounds **6** and **8a** at their IC$_{50}$ values for 24 h and their effects on the normal cell cycle profile and induction of apoptosis were recorded. Treatment of T-24 and PC-3 cells with compounds **6** and **8a** resulted in an interference with the normal distribution of the cell cycle. In T-24 cell lines, both compounds **6** and **8a** induced a significant increase in the percentage of cells at pre-G$_1$ by 16.7- and 20.1-fold, respectively when compared to the control. Also, they showed an increase in the percentage of cells in the S phase by 1.4- and 1.11-fold, sequentially compared to the control (Figures 7–9). The accumulation of cells in the pre-G1 phase indicated that CP derivatives **6** and **8a** induced tumour cell death and cytotoxicity via apoptosis. While the accumulation of the cells in the S phase might result from the cell cycle arrest of T-24 cells in the S phase.

In PC-3 cell lines, both compounds **6** and **8a** induced an increase in the percentage of cells at the G1 phase by 1.16- and 1.27-fold, respectively when compared to the control (Figures 10–12). This was confirmed by a concomitant decrease in the percentage of cells in the G2/M phase, where both compounds **6** and **8a** induced a decrease in the percentage of cells at the G2/M
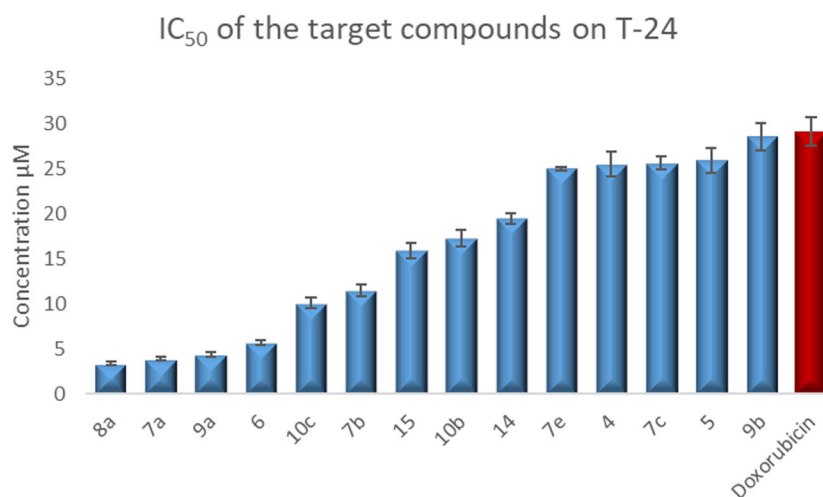
IC$_{50}$ of the target compounds on T-24

Figure 4. Graphical representation for the half-maximal inhibitory concentration (IC$_{50}$) of CP derivatives and doxorubicin after treatment for 24 h on bladder cancer cell line.
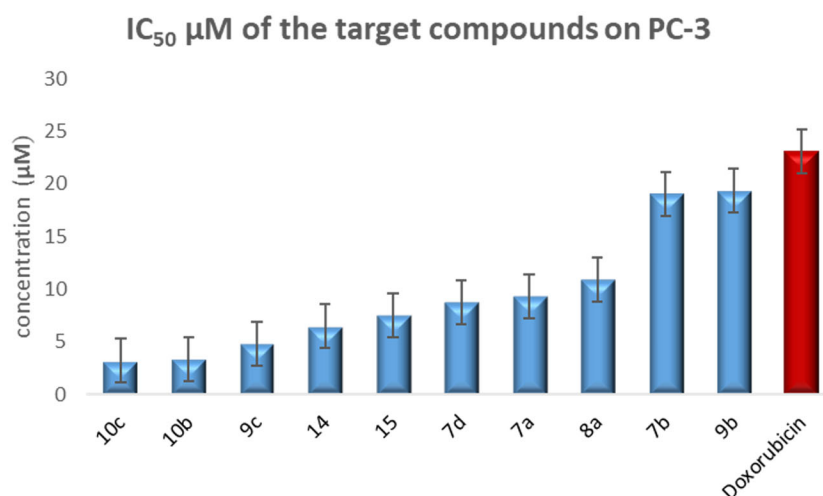
IC$_{50}$ µM of the target compounds on PC-3

Figure 5. Graphical representation for half-maximal inhibitory concentration (IC$_{50}$) of the target compounds and doxorubicin after treatment for 24 h on the prostate cancer cell line.
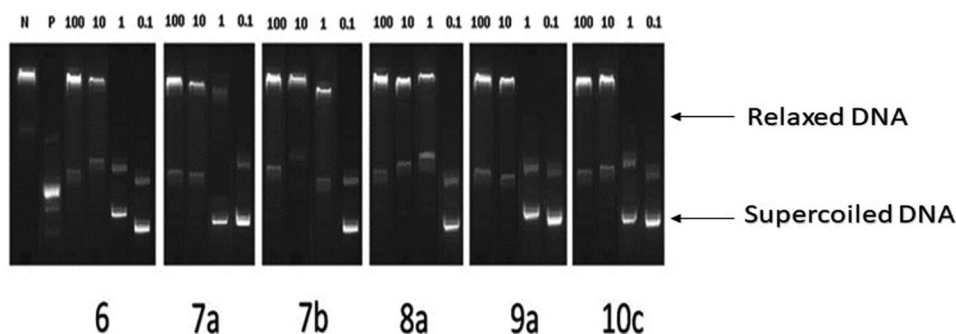

Figure 6. Recombinant Topo II inhibitory activities of compounds **6**, **7a**, **7b**, **8a**, **9a**, and **10c** at 100, 10, 1, 0.1 µM. Lane P: pBR322 DNA only; lane N: pBR322 DNA + Topo II; lanes (**6**, **7a**, **7 b**, **8a**, **9a** and **10c**): pBR322 DNA + Topo II + compounds **6**, **7a**, **7 b**, **8a**, **9a** and **10c**.

phase by 1.5- and 20.1-fold, respectively. Compounds **6** and **8a** induced G1-phase cell cycle arrest of PC-3 cells at their IC$_{50}$ concentrations. Topoisomerase inhibitors cause DNA damage which is related to G1/S and S phase arrest. Cell cycle arrest prevents the replication of damaged DNA. In PC-3 cell line compounds **6** and **8a** probably arrested the cell cycle in the G1 phase by inhibition of Cyclin D–Cdk4–Cdks complex, however in the T-24 cell line, they might arrest the cell cycle in the S phase by the inhibition of both Cyclin D–Cdk4–Cdks complex and cyclins E1–E2/Cdk2, which promote G1/S transition[66–69].

Similar effects regarding cell cycle arrest at different phases by CP derivatives have been reported, which approved that CP is a promising framework for anticancer drug design and discovery. In 2018, two CP derivatives induced a significant increase in the percentage of cells at pre-G1and G2/M phases by 13.9-, 8.8-fold, and 2.05-, 2.06-fold, respectively compared to the negative control in the UO-31 cell line[39].

Table 2. Recombinant Topo II inhibitory activities of compounds (**6**, **7a**, **7b**, **8a**, **9a**, and **10c**).

Compounds	Percentage of inhibition*			
	100 µM	10 µM	1 µM	0.1 µM
6	87.4	76.3	51.9	28.0
7a	83.6	55.9	27.9	13.7
7b	85.2	60.3	34.0	18.4
8a	91.6	77.4	50.3	32.5
9a	86.5	57.0	40.3	23.6
10c	90.2	72.6	37.7	24.8

*Percentage inhibition of Topo II activity = (Intensity of sample-treated DNA/ Intensity of vehicle-treated control DNA) × 100.

Table 3. Topo II IC_{50} results of compounds (**6**, **7a**, **7b**, **8a**, **9a**, and **10c**) compared to doxorubicin.

Compound	IC_{50} (µM*±SD)
6	0.92 ± 0.05
7a	4.99 ± 0.27
7b	3.34 ± 0.18
8a	0.74 ± 0.04
9a	2.58 ± 0.14
10c	1.69 ± 0.09
Doxorubicin	1.72 ± 0.08

*The results given are the means of three experiments.

In 2021, Abdel-Rahman et al. reported that a Mannich base CP derivative induced an increase in the percentage of cells at pre-G1and G2/M phases by 17.9- and 4.1-fold, respectively, in the OVCAR-3 cell line compared to the negative control[70].

Apoptosis determination by annexin V-FITC assay

To verify the ability of compounds **6** and **8a** to induce apoptosis, a flow cytometry assay was performed using propidium iodide (PI), and immunofluorescent markers of the protein annexin-V. Dual staining for annexin-V and with PI provides the distinction between viable cells, early apoptotic cells, late apoptotic cells, and necrotic cells[71–73]. Treatment of T-24 cells with compounds **6** and **8a** at their IC_{50} concentrations resulted in a decrease in the percentage of viable cells. The results showed that compound **6** induced both early and late apoptosis with 16.27- and 83.38-fold more than the control, respectively, and induced total apoptosis and necrosis with 16.77- and 6.25-fold more than the control, respectively (Figure 13). While compound **8a** induced both early and late apoptosis with 21.16- and 114.90-fold more than the control, respectively, and induced total apoptosis and necrosis with 20.1- and 4.28-fold more than the control, sequentially (Figure 14).

While treatment of PC-3 cells with compounds **6** and **8a** at their IC_{50} concentrations resulted in a decrease in the percentage of viable cells. The results showed that compound **6** induced both
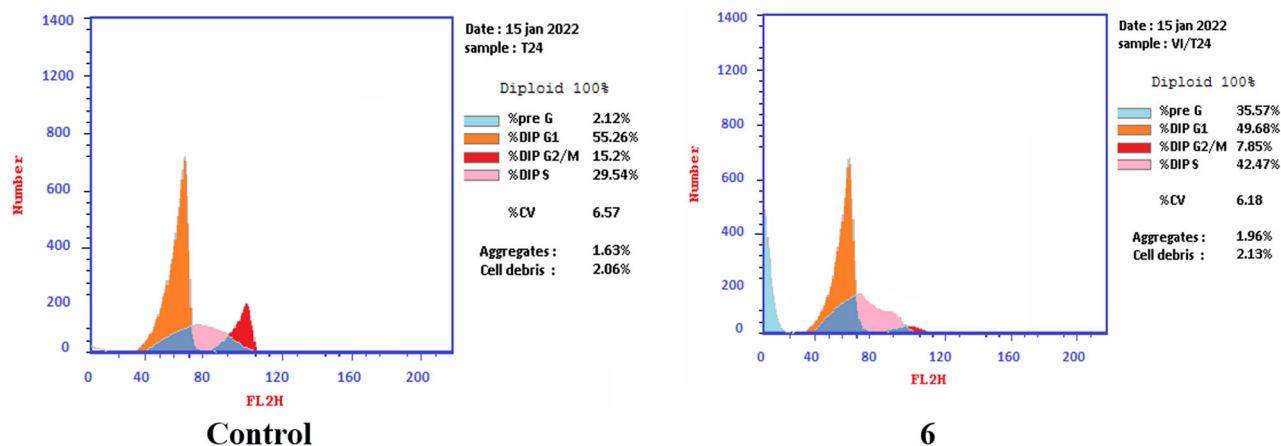
Figure 7. Effect of compound **6** (5.68 µM) on DNA-ploidy flow cytometric analysis of T-24 cells after 24 h.
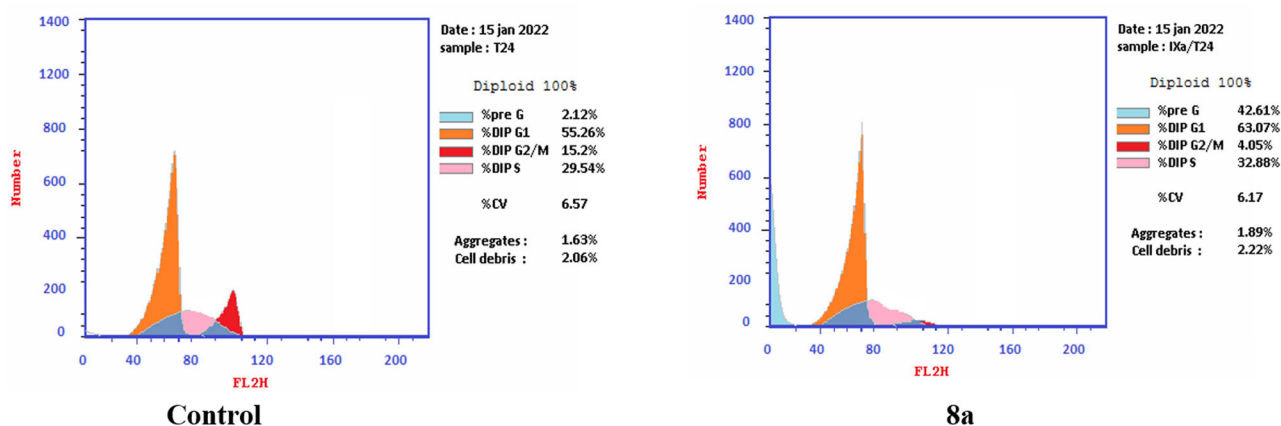
Figure 8. Effect of compound **8a** (3.36 µM) on DNA-ploidy flow cytometric analysis of T-24 cells after 24 h.

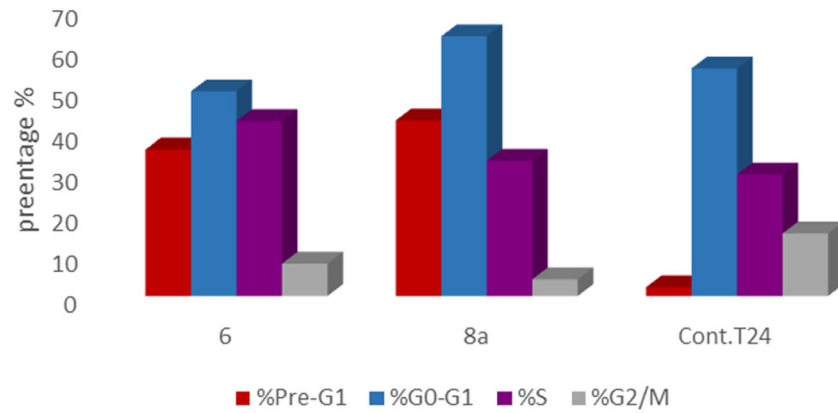## Cell Cycle analysis, T-24 cell lines
DNA content

Figure 9. Bar presentation showing effects of compounds **6** (5.68 μM) and **8a** (3.36 μM) on DNA-ploidy flow cytometric analysis of T-24 cells after 24 h.
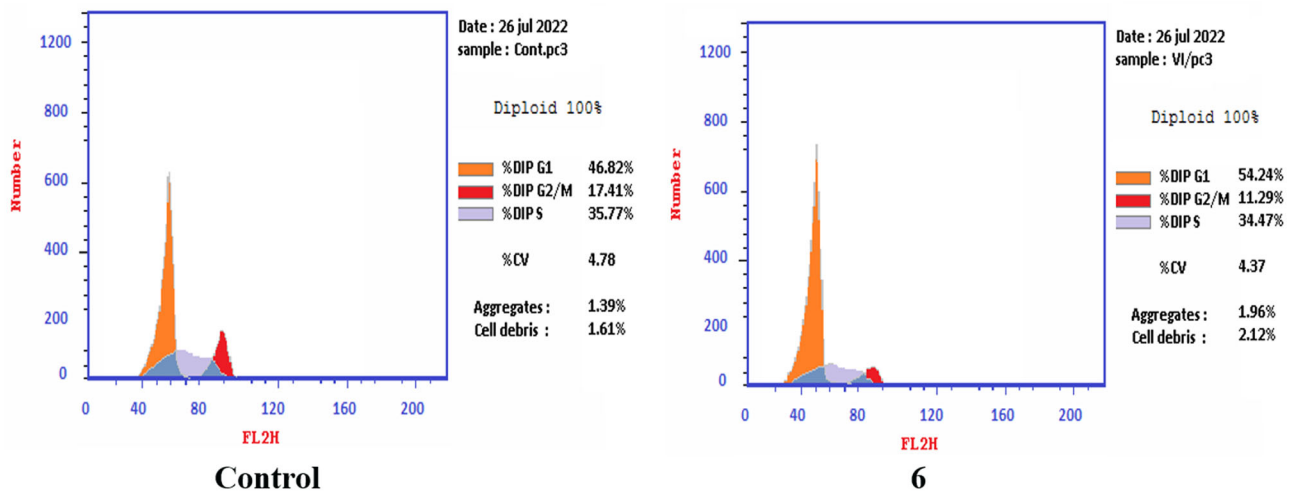

Figure 10. Effect of compound **6** (92.16 μM) on DNA ploidy flow cytometric analysis of PC-3 cells after 24 h.
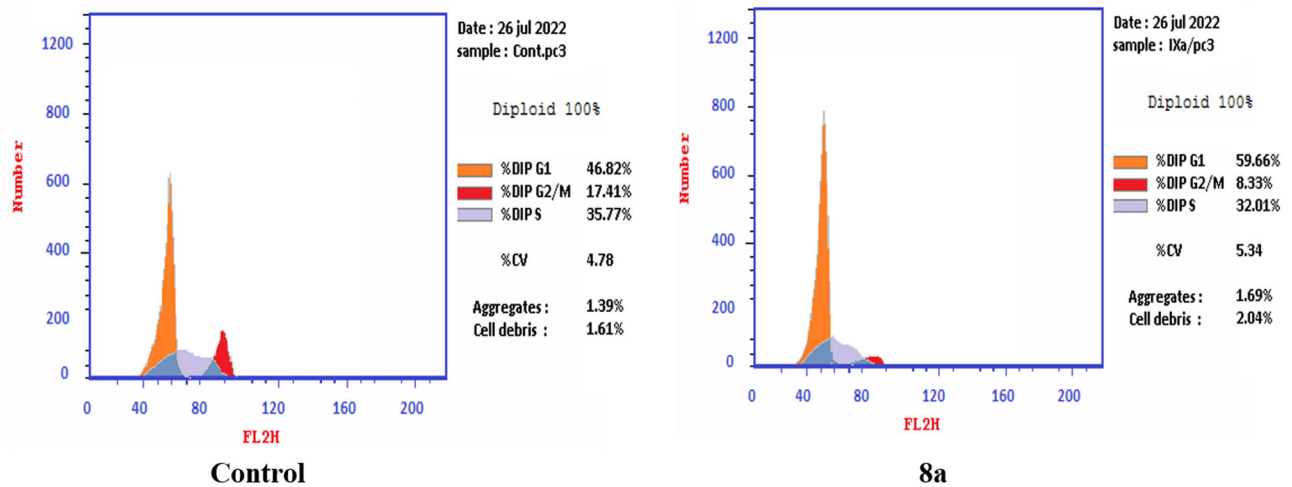

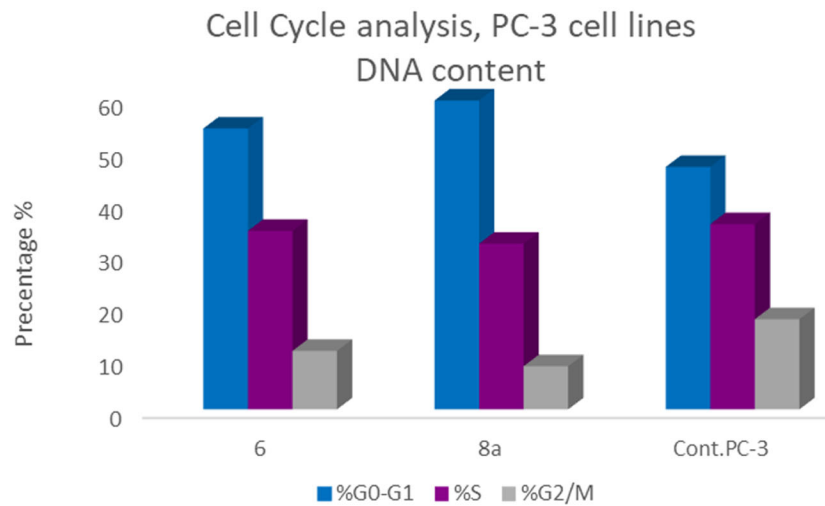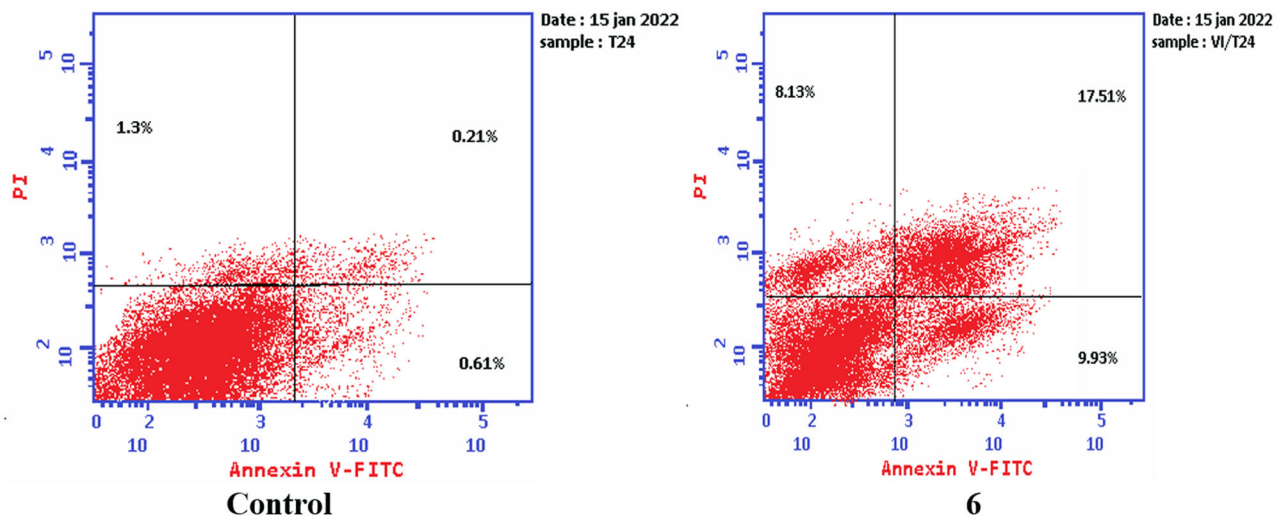**Figure 11.** Effect of compound **8a** (10.95 μM) on DNA-ploidy flow cytometric analysis of PC-3 cells after 24 h.

Figure 12. Bar presentation showing effects of compounds **6** (92.16 μM) and **8a** (10.95 μM) on DNA-ploidy flow cytometric analysis of PC-3 cells after 24 h.

Figure 13. Representative dot plots of T-24 cells treated with **6** (5.68 μM) for 24 h and analysed by flow cytometry after double staining of the cells with annexin-V FITC and PI.
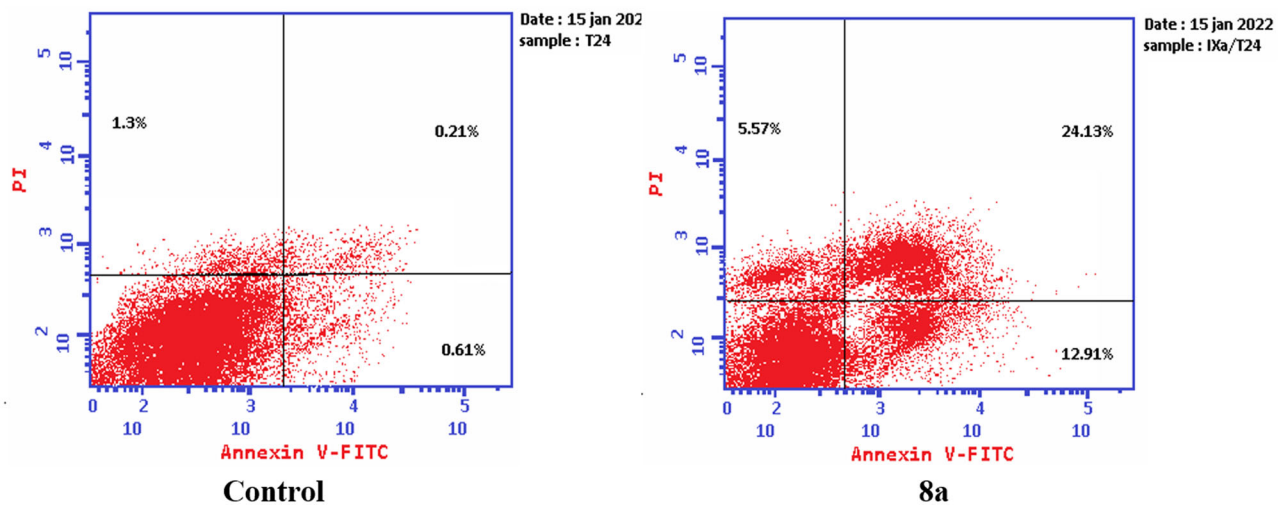

Figure 14. Representative dot plots of T-24 cells treated with **8a** (3.36 μM) for 24 h and analysed by flow cytometry after double staining of the cells with annexin-V FITC and PI.
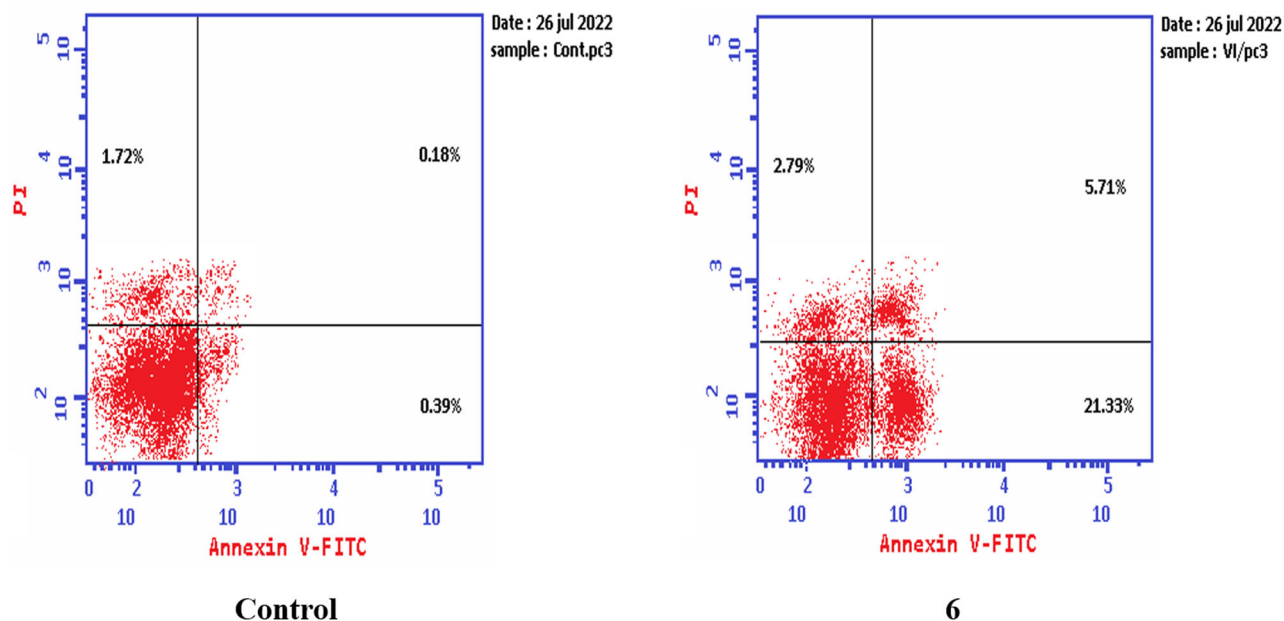
Figure 15. Representative dot plots of PC-3 cells treated with **6** (92.16 μM) for 24 h and analysed by flow cytometry after double staining of the cells with annexin-V FITC and PI.
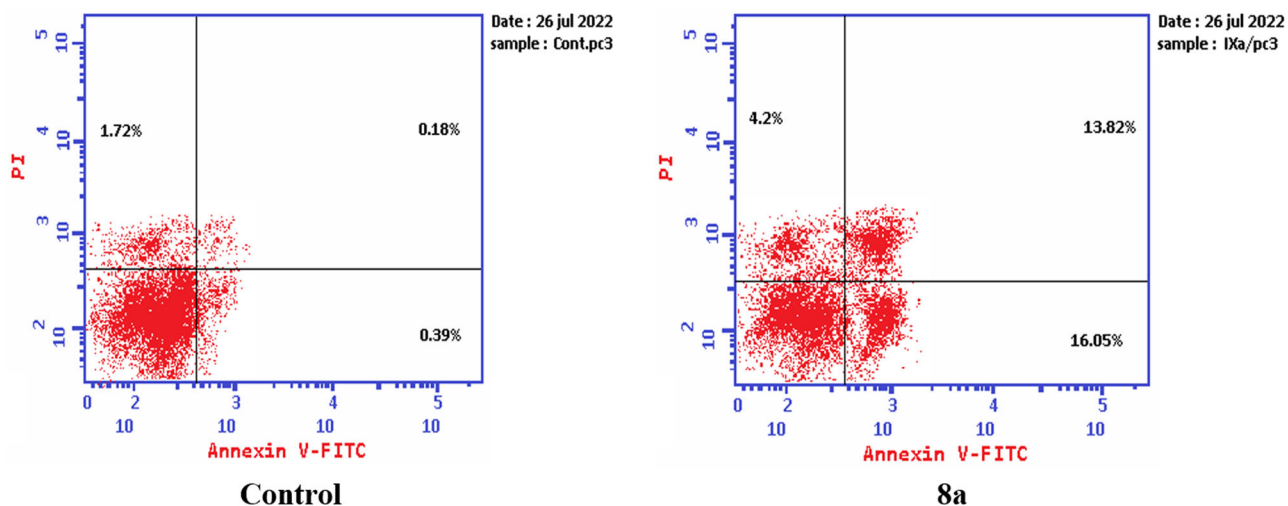

Figure 16. Representative dot plots of PC-3 cells treated with **8a** (10.95 μM) for 24 h and analysed by flow cytometry after double staining of the cells with annexin-V FITC and PI.

early and late apoptosis with 54.69- and 31.72-fold more than the control, respectively, and induced total apoptosis and necrosis with 13.02- and 1.62-fold more than the control, respectively (Figure 15). While compound **8a** induced both early and late apoptosis with 41.15- and 76.77-fold more than the control, respectively, and induced total apoptosis and necrosis with 14.87- and 2.44-fold more than the control, sequentially (Figure 16).

Effect of compounds 6 and 8a on the level of active caspase-3 (key executioner of apoptosis)

Caspase-3 (a key effector enzyme) plays an important role in apoptosis since its activation leads to catalysing specific enzymes responsible for DNA fragmentation, which leads to cell death[74–77]. Apoptosis induction in T-24 cells by compounds **6** and **8a** was investigated via caspase 3, compared to doxorubicin as a reference drug.

Treatment of T-24 cells with compounds **6** and **8a** at concentrations 5.68 and 3.36 μM, sequentially enhanced the level of

Table 4. Active caspase-3 assay results.

Compound	Caspase-3 conc. (pg/ml* ± SD)
6	362.9 ± 8.58
8a	527.6 ± 8.39
Doxorubicin	598.8 ± 8.63
Control	69.36 ± 1.70

*The results given are the means of three experiment.

active caspase-3 compared to the control (5.23- and 7.6-fold) (Table 4, Figure 17).

Molecular docking study

Docking studies were carried out for compounds **6** and **8a** which showed potent activity in the Topo II enzyme inhibition assay. We used topoisomerase IIα co-crystallised with DNA (PDB ID: 4FM9)[63] for molecular docking of compounds **6**, **8a**, and merbarone. Docking of merbarone in the DNA binding site was carried out for
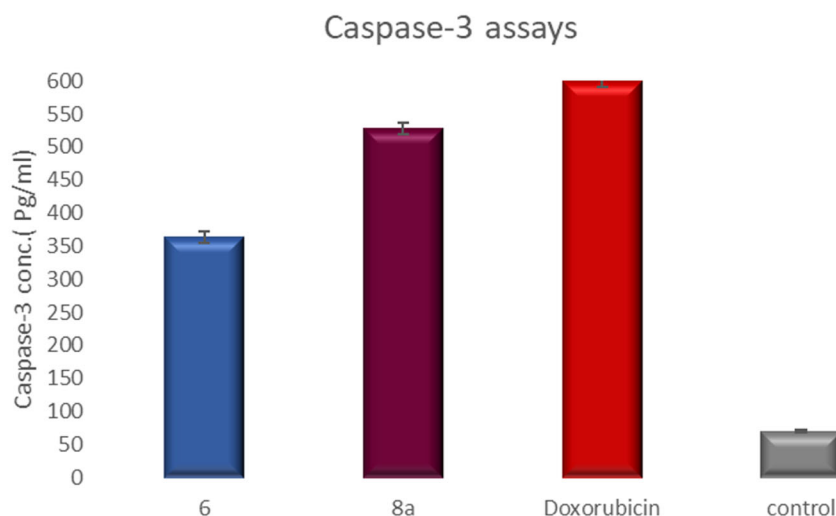
Figure 17. Graphical representation for active caspase-3 assays of compounds **6** and **8a** compared to doxorubicin as a positive control.
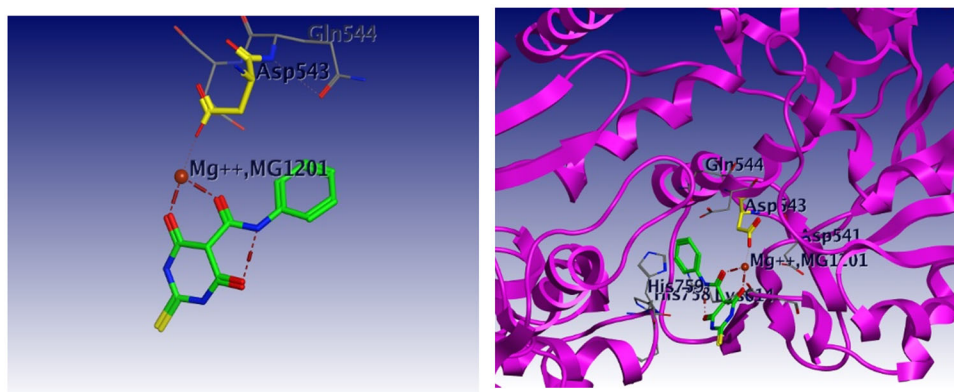

Figure 18. 3D interaction of merbarone with DNA binding site of topoisomerase IIα. Red dashed lines represent coordinate bond interactions with Mg^{2+}. Red tiny, dashed lines are hydrogen bonding interactions with amino acid Asp 543. $Mg2^{+}$ is shown as a nonbonded sphere (crimson red). Residues that are involved in hydrogen bonding are shown in the stick presentation.
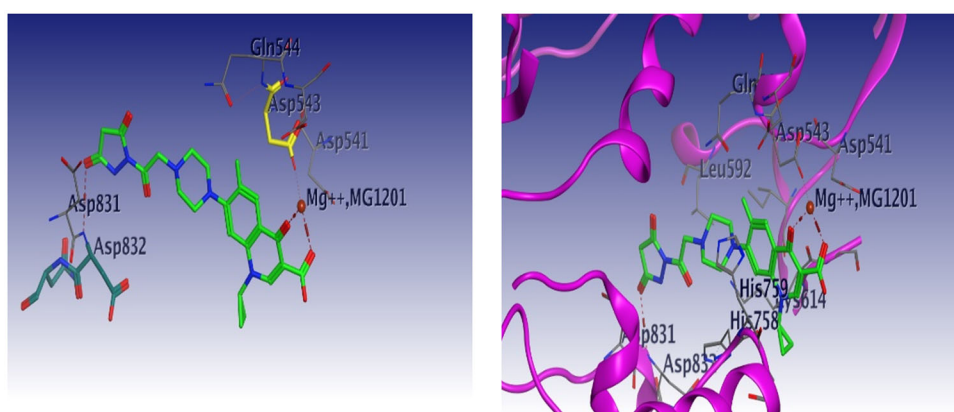

Figure 19. 3D interaction of compound **6** with DNA binding site of topoisomerase IIα. Red dashed lines represent coordinate bond interactions with Mg^{2+}. Red tiny, dashed lines are hydrogen bonding interactions with amino acid Asp 543, and Asp 831. Mg^{2+} is shown as a nonbonded sphere (crimson red). Residues that are involved in hydrogen bonding are shown in the stick presentation.

validation of the molecular docking and it was compared with a previously reported study[78]. Interestingly, the test compounds exerted favourable interactions with the Topo II enzyme active site, with almost the same binding pattern as merbarone. Merbarone showed coordinate bond interactions with Mg^{2+} and H-bond interaction with amino acid Asp 543 (Figure 18).

Compound **6** interacted in a similar pattern, the oxygen atoms of both coplanar carbonyl groups at positions 3 and 4 formed coordinate bond interactions with Mg^{2+} and H-bond interaction with amino acid Asp 543. Moreover, compound **6** interacted as an H-bond acceptor through the carbonyl group of its pyrazolidine moiety with amino acid Asp 831(Figure 19). Regarding compound
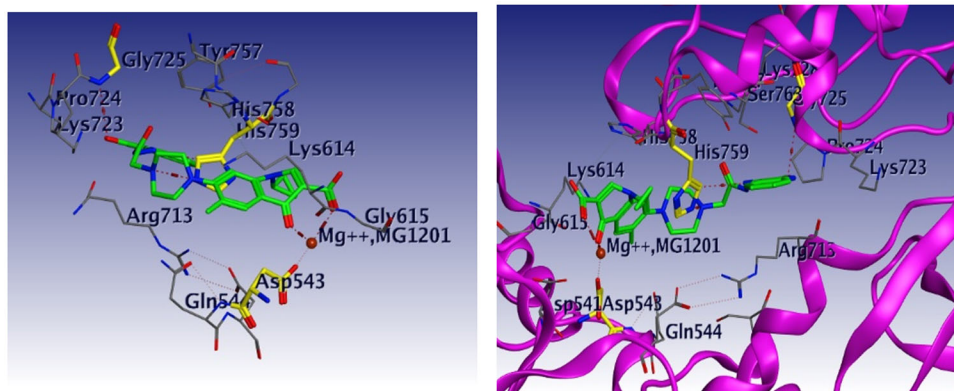
Figure 20. 3D interaction of compound **8a** with DNA binding site of topoisomerase IIα. Red dashed lines represent coordinate bond interactions with Mg^{2+}. Red tiny, dashed lines are hydrogen bonding interactions with amino acid Asp 543, acids His 759 and Gly 725. Mg^{2+} is shown as a nonbonded sphere (crimson red). Residues that are involved in hydrogen bonding are shown in the stick presentation.

8a, it interacted with the Topo II enzyme through coordinate bonding with the magnesium ion Mg^{2+} via the oxygen atoms of both carbonyl groups at positions 3 and 4 and H-bond interaction with amino acid Asp 543. Additionally, it interacted as an H-bond acceptor with amino acids His 759 and Gly 725 through the N atom of piperazine and carbonyl group of indoline moiety, respectively. It exerted arene cation interaction with Arg 713 (Figure 20).

Conclusion

In summary, a series of novel CP derivatives were designed and synthesised. They were evaluated for their anti-proliferative activity against bladder T-24 and prostate PC-3 cancer cell lines. 14 compounds exhibited potent antiproliferative activity against the T-24 cell line, with IC_{50} values between 3.36 and 28.55 μM, which was 1.02- to 8.66-fold more potent than the reference drug doxorubicin. 10 compounds proved their potency against the PC-3 cell line with IC_{50} values between 3.24 and 19.33 μM, which was 1.2- to 7.1-fold more potent than doxorubicin. The most potent compounds **6**, **7a**, **7b**, **8a**, **9a**, and **10c** showed significant Topo II inhibitory activity. Compounds **6**, **8a**, and **10c** were 1.01- to 2.32-fold more potent than doxorubicin. The most prominent compounds **6** and **8a** were further investigated regarding their effects on cell cycle progression, induction of apoptosis, and level of active caspase-3 in the T-24 and PC-3 cell lines. Both compounds induced apoptosis in T-24 cells (16.8- and 20.1-fold, respectively compared to control). This evidence was supported by an increase in the level of apoptotic caspase-3 (5.23- and 7.6-fold). Compounds **6** and **8a** arrested the cell cycle in the S phase. Regarding the induction of apoptosis in PC-3 cell lines, both compounds **6** and **8a** induced G1-phase cell cycle arrest at their IC_{50} concentrations. This was confirmed by the increase in the percentage of cells in the G1 phase (1.16- and 1.27-fold, respectively), and a concomitant decrease in the percentage of cells in G2/M phase, (1.5- and 20.1-fold, respectively). The treatment of PC-3 cells with compounds **6** and **8a** at their IC_{50} concentrations resulted in a decrease in the percentage of viable cells. The results showed that both compounds **6** and **8a** induced both early and late apoptosis. The molecular docking study of these compounds with Topo II protein revealed more favourable binding modes compared to merbarone, explaining their remarkable Topo II inhibitory potency. CP derivatives are promising leads for further studying, designing, and synthesis of potent anti-proliferative candidates.

Disclosure statement

Funding

References

1. World Health Organization. Cancer [Internet]. Geneva (Switzerland): WHO; 2021 [cited 2022 Feb 3]. Available from: https://www.who.int/news-room/fact-sheets/detail/cancer.
2. Norman A. On the origin of cancer foci. Cancer. 1952;5(3): 581–582.
3. Biller LH, Schrag D. Diagnosis and treatment of metastatic colorectal cancer: a review. JAMA. 2021;325(7):669–685.
4. Mansoori B, Mohammadi A, Davudian S, Shirjang S, Baradaran B. The different mechanisms of cancer drug resistance: a brief review. Adv Pharm Bull. 2017;7(3):339–348.
5. Nitiss JL, Kiianitsa K, Sun Y, Nitiss KC, Maizels N. Topoisomerase assays. Curr Protoc. 2021;1(10):e250.
6. Lee JH, Berger JM. Cell cycle-dependent control and roles of DNA topoisomerase II. Genes. 2019;10(11):859.
7. Baguley BC, Drummond CJ, Chen YY, Finlay GJ. DNA-binding anticancer drugs: one target, two actions. Molecules. 2021; 26(3):552.
8. Sissi C, Palumbo M. Effects of magnesium and related divalent metal ions in topoisomerase structure and function. Nucleic Acids Res. 2009;37(3):702–711.
9. Lehninger A, Nelson DL, Cox MM. Biochemistry principles. 7th ed. New York: W.H. Freeman; 2017. p. 1328.
10. Delgado JL, Hsieh C-M, Chan N-L, Hiasa H. Topoisomerases as anticancer targets. Biochem J. 2018;475(2):373–398.
11. Hevener KE, Verstak TA, Lutat KE, Riggsbee DL, Mooney JW. Recent developments in topoisomerase-targeted cancer chemotherapy. Acta Pharm Sin B. 2018;8(6):844–861.
12. Buzun K, Bielawska A, Bielawski K, Gornowicz A. DNA topoisomerases as molecular targets for anticancer drugs. J Enzyme Inhib Med Chem. 2020;35(1):1781–1799.
13. Skok Z, Zidar N, Kikelj D, Ilas J. Dual inhibitors of human DNA topoisomerase II and other cancer- related targets. J Med Chem. 2020;63(3):884–904.

14. Johnson-Arbor K, Dubey R. Doxorubicin. In: StatPearls [Internet]. Treasure Island (FL): StatPearls Publishing; 2022. PMID: 29083582.

15. Abdel-Aal MAA, Abdel-Aziz SA, Shaykoon MSA, Abuo-Rahma GEDA. Towards anticancer fluoroquinolones: a review article. Arch Pharm. 2019;352(7):e1800376.

16. Ezelarab HAA, Abbas SH, Hassan HA, Abuo-Rahma GEDA. Recent updates of fluoroquinolones as antibacterial agents. Arch Pharm Chem Life Sci. 2018;351(9):1800141.

17. Yadav V, Talwar P. Repositioning of fluoroquinolones from antibiotic to anti-cancer agents: an underestimated truth. Biomed Pharmacother. 2019;111:934–946.

18. Kathiravan MK, Khilare MM, Nikoomanesh K, Aparna S, Jain KS. Topoisomerase as target for antibacterial and anticancer drug discovery. J Enzyme Inhib Med Chem. 2013;28(3):419–435.

19. Idowu T, Schweizer F. Ubiquitous nature of fluoroquinolones: the oscillation between antibacterial and anticancer activities. Antibiotics. 2017;6(4):26.

20. Gouvea LR, Garcia LS, Lachter DR, Nunes PR, de Castro Pereira F, Silveira-Lacerda EP, Louro SRW, Barbeira PJS, Teixeira LR. Atypical fluoroquinolone gold(III) chelates as potential anticancer agents: relevance of DNA and protein interactions for their mechanism of action. Eur J Med Chem. 2012;55:67–73.

21. Samir M, Ramadan M, Hamed M, Osman M, Abou-Rahma G. Recent strategies in design of antitumor and antibacterial fluoroquinolones. J Adv Biomed Pharm Sci. 2021;4(3):134–151.

22. Bisacchi GS, Hale MR. A "double-edged" scaffold: antitumor power within the antibacterial quinolone. Curr Med Chem. 2016;23(6):520–577.

23. Wang L-L, Battini N, Rammohan RY, Bheemanaboina S-L, Zhang CHZ. Design and synthesis of aminothiazolyl norfloxacin analogues as potential antimicrobial agents and their biological evaluation. Eur J Med Chem. 2019;167:105–123.

24. Kloskowski T, Szeliski K, Fekner Z, Rasmus M, Paweł D, Wolska A. Ciprofloxacin and levofloxacin as potential drugs in genitourinary cancer treatment – the effect of dose-response on 2d and 3d cell cultures. Int J Mol Sci. 2021; 22(21):11970.

25. Gupta P, Gao HL, Ashar YV, Karadkhelkar NM, Yoganathan S, Chen ZS. Ciprofloxacin enhances the chemosensitivity of cancer cells to ABCB1 substrates. Int J Mol Sci. 2019;20(2):268.

26. Herold C, Ocker M, Ganslmayer M, Gerauer H, Hahn EG, Schuppan D. Ciprofloxacin induces apoptosis and inhibits proliferation of human colorectal carcinoma cells. Br J Cancer. 2002;86(3):443–448.

27. Yadav V, Varshney P, Sultana S, Yadav J, Saini N. Moxifloxacin and ciprofloxacin induces S-phase arrest and augments apoptotic effects of cisplatin in human pancreatic cancer cells via ERK activation. BMC Cancer. 2015;15(1):1–15.

28. Liu H, Huang J, Wang J, Wang M, Liu M, Wang B, Guo H, Lu Y. Synthesis, antimycobacterial and antibacterial evaluation of I-[(1R, 2S)-2-fluorocyclopropyl]fluoroquinolone derivatives containing an oxime functional moiety. Eur J Med Chem. 2014;86:628–638.

29. Mohammadhosseini N, Alipanahi Z, Alipour E, Emami S, Faramarzi MA, Samadi N, Khoshnevis N, Shafiee A, Foroumadi A. Synthesis and antibacterial activity of novel levofloxacin derivatives containing a substituted thienylethyl moiety. DARU. 2012;20(1):1.

30. Gao F, Zhang X, Wang T, Xiao J. Quinolone hybrids and their anti-cancer activities: an overview. Eur J Med Chem. 2019; 165:59–79.

31. Zhang GF, Zhang S, Pan B, Liu X, Feng LS. 4-Quinolone derivatives and their activities against Gram positive pathogens. Eur J Med Chem. 2018;143:710–723.

32. Sissi C, Palumbo M. The quinolone family: from antibacterial to anticancer agents. Curr Med Chem Anticancer Agents. 2003;3(6):439–450.

33. Suaifan GARY, Mohammed AAM. Fluoroquinolones structural and medicinal developments (2013–2018): where are we now? Bioorg Med Chem. 2019;27(14):3005–3060.

34. Liu J, Ren Z, Fan L, Wei J, Tang X, Xu X, Yang D. Design, synthesis, biological evaluation, structure-activity relationship, and toxicity of clinafloxacin-azole conjugates as novel antitubercular agents. Bioorg Med Chem. 2019;27(1):175–187.

35. Feng L, Lv K, Liu M, Wang S, Zhao J, You X, Li S, Cao J, Guo H. Synthesis and in vitro antibacterial activity of gemifloxacin derivatives containing a substituted benzyloxime moiety. Eur J Med Chem. 2012;55:125–136.

36. Zhang YB, Feng LS, You XF, Guo Q, Guo HY, Liu ML. Synthesis and in vitro antibacterial activity of 7-(3-alkoxyimino-4-methyl-4-methylaminopiperidin-1-yl)-fluoroquinolone derivatives. Arch Pharm. 2010;343(3):143–151.

37. Abuo-Rahma GDAA, Sarhan HA, Gad GFM. Design, synthesis, antibacterial activity and physicochemical parameters of novel N-4-piperazinyl derivatives of norfloxacin. Bioorg Med Chem. 2009;17(11):3879–3886.

38. Alovero FL, Pan XS, Morris JE, Manzo RH, Fisher LM. Engineering the specificity of antibacterial fluoroquinolones: benzenesulfonamide modifications at C-7 of ciprofloxacin change its primary target in Streptococcus pneumoniae from topoisomerase IV to gyrase. Antimicrob Agents Chemother. 2000;44(2):320–325.

39. Kassab AE, Gedawy EM. Novel ciprofloxacin hybrids using biology oriented drug synthesis (BIODS) approach: anticancer activity, effects on cell cycle profile, caspase-3 mediated apoptosis, topoisomerase II inhibition, and antibacterial activity. Eur J Med Chem. 2018;150:403–418.

40. Khélifa T, Beck WT. Merbarone, a catalytic inhibitor of DNA topoisomerase II, induces apoptosis in CEM cells through activation of ICE/CED-3-like protease. Mol Pharmacol. 1999; 55(3):548–556.

41. Hotinski AK, Lewis ID, Ross DM. Vosaroxin is a novel topoisomerase-II inhibitor with efficacy in relapsed and refractory acute myeloid leukaemia. Expert Opin Pharmacother. 2015; 16(9):1395–1402.

42. Kohlbrenner WE, Wideburg N, Weigl D, Saldivar A, Chu DTW. Induction of calf thymus topoisomerase II-mediated DNA breakage by the antibacterial isothiazoloquinolones A-65281 and A-65282. Antimicrob Agents Chemother. 1992;36(1):81–86.

43. Chauhan S, Paliwal S, Chauhan R. Anticancer activity of pyrazole via different biological mechanisms. Synth Commun. 2014;44(10):1333–1374.

44. Luzina EL, Popov AV. Synthesis and anticancer activity evaluation of 3,4-mono- and bicyclosubstituted N-(het)aryl trifluoromethyl succinimides. J Fluor Chem. 2014;168:121–127.

45. Milosevic NP, Kojic V, Curcic J, Jakimov D, Milic N, Banjac N, Uscumlic G, Kaliszan R. Evaluation of in silico pharmacokinetic properties and in vitro cytotoxic activity of selected newly synthesized N-succinimide derivatives. J Pharm Biomed Anal. 2017;137:252–257.

46. Tan A, Yaglioglu AS, Kishali NH, Sahin E, Kara Y. Evaluation of cytotoxic potentials of some isoindole-1,3-dione derivatives on HeLa, C6 and A549 cancer cell lines. Med Chem. 2020;16(1):69–77.

47. Firoozpour L, Gao L, Moghimi S, Pasalar P, Davoodi J, Wang M-W, Rezaei Z, Dadgar A, Yahyavi H, Amanlou M, et al. Efficient synthesis, biological evaluation, and docking study of isatin based derivatives as caspase inhibitors. J Enzyme Inhib Med Chem. 2020;35(1):1674–1684.

48. Ma L, Wang H, Wang J, Liu L, Zhang S, Bu M. Novel steroidal 5α,8α-endoperoxide derivatives with semicarbazone/thiosemicarbazone side-chain as apoptotic inducers through an intrinsic apoptosis pathway: design, synthesis and biological studies. Molecules. 2020;25(5):1209.

49. Muğlu H. Synthesis, characterization, and antioxidant activity of some new N4-aryl substituted-5-methoxyisatin-β-thiosemicarbazone derivatives. Res Chem Intermed. 2020;46(4):2083–2098.

50. El Majzoub R, Fayyad-Kazan M, Nasr El Dine A, Makki R, Hamade E, Grée R, Hachem A, Talhouk R, Fayyad-Kazan H, Badran B, et al. A thiosemicarbazone derivative induces triple negative breast cancer cell apoptosis: possible role of miRNA-125a-5p and miRNA-181a-5p. Genes Genomics. 2019;41(12):1431–1443.

51. Hsu DC, Roth HS, West DC, Botham RC, Novotny CJ, Schmid SC, Hergenrother PJ. Parallel synthesis and biological evaluation of 837 analogues of procaspase-activating compound 1 (PAC-1). ACS Comb Sci. 2012;14(1):44–50.

52. Liang Z, Zhang D, Ai J, Chen L, Wang H, Kong X, Zheng M, Liu H, Luo C, Geng M, et al. Identification and synthesis of N′-(2-oxoindolin-3-ylidene)hydrazide derivatives against c-Met kinase. Bioorg Med Chem Lett. 2011;21(12):3749–3754.

53. Hantgan RR, Stahle MC. Integrin priming dynamics: mechanisms of integrin antagonist-promoted αIIbβ3:PAC-1 molecular recognition. Biochemistry. 2009;48(35):8355–8365.

54. Kasiotis KM, Tzanetou EN, Haroutounian SA. Pyrazoles as potential anti-angiogenesis agents: a contemporary overview. Front Chem. 2014;2:78–77.

55. Awadallah FM, Piazza GA, Gary BD, Keeton AB, Canzoneri JC. Synthesis of some dihydropyrimidine-based compounds bearing pyrazoline moiety and evaluation of their antiproliferative activity. Eur J Med Chem. 2013;70:273–279.

56. Rathore P, Yaseen S, Ovais S, Bashir R, Yaseen R, Hameed AD, Samim M, Gupta R, Hussain F, Javed K, et al. Synthesis and evaluation of some new pyrazoline substituted benzenesulfonylureas as potential antiproliferative agents. Bioorg Med Chem Lett. 2014;24(7):1685–1691.

57. George RF, Fouad MA, Gomaa IEO. Synthesis and cytotoxic activities of some pyrazoline derivatives bearing phenyl pyridazine core as new apoptosis inducers. Eur J Med Chem. 2016;112:48–59.

58. Fahmy HH, Khalifa NM, Ismail MMF, El-Sahrawy HM, Nossier ES. Biological validation of novel polysubstituted pyrazole candidates with in vitro anticancer activities. Molecules. 2016;21(3):271.

59. Best J, Schotten C, Lohmann G, Gerken G, Dechêne A. Tivantinib for the treatment of hepatocellular carcinoma. Expert Opin Pharmacother. 2017;18(7):727–733.

60. Devi KS, Subramani P, Parthiban S, Sundaraganesan N. One-pot synthesis, spectroscopic characterizations, quantum chemical calculations, docking and cytotoxicity of 1-((dibenzylamino)methyl)pyrrolidine-2,5-dione. J Mol Struct. 2020;1203:127403.

61. Han SH, Kim S, De U, Mishra NK, Park J, Sharma S, Kwak JH, Han S, Kim HS, Kim IS, et al. Synthesis of succinimide-containing chromones, naphthoquinones, and xanthones under Rh(III) catalysis: evaluation of anticancer activity. J Org Chem. 2016;81(24):12416–12425.

62. Mitra I, Mukherjee S, Reddy BVP, Dasgupta S, Bose KJC, Mukherjee S, Linert W, Moi SC. Benzimidazole based Pt(II) complexes with better normal cell viability than cisplatin: synthesis, substitution behavior, cytotoxicity, DNA binding and DFT study. RSC Adv. 2016;6(80):76600–76613.

63. Wendorff TJ, Schmidt BH, Heslop P, Austin CA, Berger JM. The structure of DNA-bound human topoisomerase II alpha: conformational mechanisms for coordinating inter-subunit interactions with DNA cleavage. J Mol Biol. 2012;424(3–4):109–124.

64. Protein Data Bank. Available from: http://www.rcsb.org/pdb.

65. Vincenzi B, Frezza AM, Santini D, Tonini G. New therapies in soft tissue sarcoma. Expert Opin Emerg Drugs. 2010;15(2):237–248.

66. Poli A, Mongiorgi S, Cocco L, Follo MY. Protein kinase C involvement in cell cycle modulation. Biochem Soc Trans. 2014;42(5):1471–1476.

67. Chen Y-J, Dominguez-Brauer C, Wang Z, Asara JM, Costa RH, Tyner AL, Lau LF, Raychaudhuri P. A conserved phosphorylation site within the forkhead domain of FoxM1B is required for its activation by cyclin-CDK1. J Biol Chem. 2009;284(44):30695–30707.

68. Black AR, Black JD. Protein kinase C signaling and cell cycle regulation. Front Immunol. 2012;3:423.

69. Ding L, Cao J, Lin W, Chen H, Xiong X, Ao H, Yu M, Lin J, Cui Q. The roles of cyclin-dependent kinases in cell-cycle progression and therapeutic strategies in human breast cancer. Int J Mol Sci. 2020;21(6):1960.

70. Abdel-Rahman IM, Mustafa M, Mohamed SA, Yahia R, Abdel-Aziz M, Abuo-Rahma GE-DA, Hayallah AM. Novel Mannich bases of ciprofloxacin with improved physicochemical properties, antibacterial, anticancer activities and caspase-3 mediated apoptosis. Bioorg Chem. 2021;107:104629.

71. D'Arcy MS. Cell death: a review of the major forms of apoptosis, necrosis and autophagy. Cell Biol Int. 2019;43(6):582–592.

72. Obeng E. Apoptosis (programmed cell death) and its signals - a review. Braz J Biol. 2021;81(4):1133–1143.

73. Majtnerová P, Roušar T. An overview of apoptosis assays detecting DNA fragmentation. Mol Biol Rep. 2018;45(5):1469–1478.

74. Araya LE, Soni IV, Hardy JA, Julien O. Deorphanizing caspase-3 and caspase-9 substrates in and out of apoptosis with deep substrate profiling. ACS Chem Biol. 2021;16(11):2280–2296.

75. Mai F-Y, He P, Ye J-Z, Xu L-H, Ouyang D-Y, Li C-G, Zeng Q-Z, Zeng C-Y, Zhang C-C, He X-H, et al. Caspase-3-mediated GSDME activation contributes to cisplatin- and doxorubicin-induced secondary necrosis in mouse macrophages. Cell Prolif. 2019;52(5):e12663.

76. Jeelani R, Chatzicharalampous C, Kohan-Ghadr H-R, Bai D, Morris RT, Sliskovic I, Awonuga A, Abu-Soud HM. Hypochlorous acid reversibly inhibits caspase-3: a potential regulator of apoptosis. Free Radic Res. 2020;54(1):43–56.

77. Beroske L, Van den Wyngaert T, Stroobants S, Van der Veken P, Elvas F. Molecular imaging of apoptosis: the case of caspase-3 radiotracers. Int J Mol Sci. 2021;22(8):3948.

78. Baviskar AT, Amrutkar SM, Trivedi N, Chaudhary V, Nayak A, Guchhait SK, Banerjee UC, Bharatam PV, Kundu CN. Switch in site of inhibition: a strategy for structure-based discovery of human topoisomerase IIα catalytic inhibitors. ACS Med Chem Lett. 2015;6(4):481–485.